

# Efficient tools for quantum metrology with uncorrelated noise

Jan Kołodyński and Rafał Demkowicz-Dobrzański

Faculty of Physics, University of Warsaw, 00-681 Warszawa, Poland

E-mail: jankolo@fuw.edu.pl and demko@fuw.edu.pl

**Abstract.** Quantum metrology offers an enhanced performance in experiments such as gravitational wave-detection, magnetometry or atomic clocks frequency calibration. The enhancement, however, requires a delicate tuning of relevant quantum features such as entanglement or squeezing. For any practical application the inevitable impact of decoherence needs to be taken into account in order to correctly quantify the ultimate attainable gain in precision. We compare the applicability and the effectiveness of various methods of calculating the ultimate precision bounds resulting from the presence of decoherence. This allows us to put a number of seemingly unrelated concepts into a common framework and arrive at an explicit hierarchy of quantum metrological methods in terms of the tightness of the bounds they provide. In particular, we show a way to extend the techniques originally proposed in Demkowicz-Dobrzański R, Kołodyński J and Guță M 2012 *Nat. Commun.* **3** 1063, so that they can be efficiently applied not only in the asymptotic but also in the finite-number of particles regime. As a result, we obtain a simple and direct method, yielding bounds that interpolate between the quantum enhanced scaling characteristic for small number of particles and the asymptotic regime, where quantum enhancement amounts to a constant factor improvement. Methods are applied to numerous models including noisy phase and frequency estimation, as well as the estimation of the decoherence strength itself.

PACS numbers: 03.67.-a, 03.65.Yz, 03.65.Ud, 03.65.Ta, 42.50.St

# Contents

<b>1</b>	<b>Introduction</b>	<b>4</b>
<b>2</b>	<b>Quantum Fisher Information</b>	<b>7</b>
2.1	Classical Cramér-Rao bound . . . . .	7
2.2	Quantum Cramér-Rao bound . . . . .	7
2.3	Purification-based definition of QFI . . . . .	8
2.4	Right logarithmic derivative (RLD)-based upper bound on QFI . . . . .	9
<b>3</b>	<b>Estimation of a quantum channel</b>	<b>9</b>
3.1	Channel QFI . . . . .	9
3.2	Purification-based definition of channel QFI . . . . .	10
3.3	Extended channel QFI . . . . .	11
3.4	RLD-based upper bound on extended channel QFI . . . . .	12
<b>4</b>	<b>Estimation of <math>N</math> independent quantum channels</b>	<b>13</b>
4.1	Standard quantum limit (SQL)-like bounds on precision in the asymptotic $N$ limit . . . . .	14
4.1.1	Classical simulation (CS) method . . . . .	15
4.1.2	Quantum simulation (QS) method . . . . .	15
4.1.3	Channel extension (CE) method . . . . .	17
4.2	Finite- $N$ channel extension (CE) method . . . . .	18
<b>5</b>	<b>Frequency estimation in atomic models</b>	<b>21</b>
<b>6</b>	<b>Estimation of decoherence strength</b>	<b>22</b>
<b>7</b>	<b>Further discussion</b>	<b>24</b>
<b>8</b>	<b>Summary and outlook</b>	<b>25</b>
	<b>Acknowledgements</b>	<b>25</b>
	<b>Appendix A Channels considered</b>	<b>26</b>
Appendix A.1	Dephasing . . . . .	26
Appendix A.2	Depolarization . . . . .	26
Appendix A.3	Loss . . . . .	27
Appendix A.4	Spontaneous emission (amplitude damping) . . . . .	28
	<b>Appendix B Equivalence of RLD-based bound applicability and local classical simulability of a channel</b>	<b>28</b>
	<b>Appendix C RLD-based bound as a special case of asymptotic CE bound</b>	<b>29</b>

Appendix D Optimal local QS of a channel 30

Appendix E Finite- $N$  CE method as a semi-definite programming task 31

## 1. Introduction

Quantum enhanced metrology has recently enjoyed a great success at experimental level leading to new results in atomic spectroscopy [1–4], magnetometry [5–7] and optical interferometry [8–11] with prominent achievements in gravitational waves sensing [12]. As predicted in the incipient theoretical results of [13–17], a physical parameter unitarily encoded into a quantum system—a probe—consisting of  $N$  entangled, non-interacting particles (atoms or photons) can be extracted with a precision that is limited by the quantum-mechanical uncertainty relations and not the more restrictive central limit theorem of classical statistics. Hence, the uncertainty in reconstructing the encoded parameter, such as e.g. optical phase delay or frequency difference, can in principle be proportional to  $1/N$ , the so-called *Heisenberg Limit* (HL), rather than  $1/\sqrt{N}$ , commonly referred to as the *Standard Quantum Limit* (SQL) or the shot (projection) noise. However, this dramatic scaling improvement can be illusive, as both the experimental results and theoretical toy-models have indicated that achieving the ideal HL is a hard task owing to the strong destructive impact of imperfections, which should be always accounted for in realistic scenarios.

An important question that has been considerably addressed by many researchers [18–32] reads: how and to what extent can the noise effects be compensated in quantum metrological setups? In the case of atomic spectroscopy, it has already been indicated in [24, 25] that the effects of uncorrelated noise, independently affecting the atoms within a probe, have a dramatic impact on quantum protocols—most likely restricting the ultimate precision scaling to become SQL-like for high enough  $N$ , so that the quantum enhancement is asymptotically limited to a multiplicative *constant factor*. In optical interferometry, photonic loss is the main obstacle to practical implementations of quantum enhanced protocols [27–30] and the asymptotic SQL-like scaling is again inevitable, as proven in [31, 32]. Similarly to the atomic case, the asymptotic improvement constant becomes an essential feature which determines the achievable precision for high  $N$ . Following the above exemplary models, methods of quantifying the asymptotic quantum enhancement have been proposed for arbitrary kinds of probes with decoherence present [33–39]. Recently, general procedures have been established that are capable of deriving practical bounds on ultimate achievable precision in realistic quantum metrological setups [38, 39]. In particular, in the case of uncorrelated noise it has been demonstrated that the sole analysis of the evolution of a *single* particle often leads to surprisingly informative bounds on the precision achievable with arbitrarily entangled multi-particle inputs [39]—see Figure 1 for an outline of a relevant metrological scheme and a summary of the single particle (single channel) methods investigated further on in this paper. For completeness, it should be noted that there are some specific metrological models *with* noise, in which asymptotic scaling power enhancement *is* nevertheless possible [22, 23, 40]. Still, applicability of these models is limited, since in any practical implementation the noise types considered will always be accompanied by some generic decoherence processes for which the constant

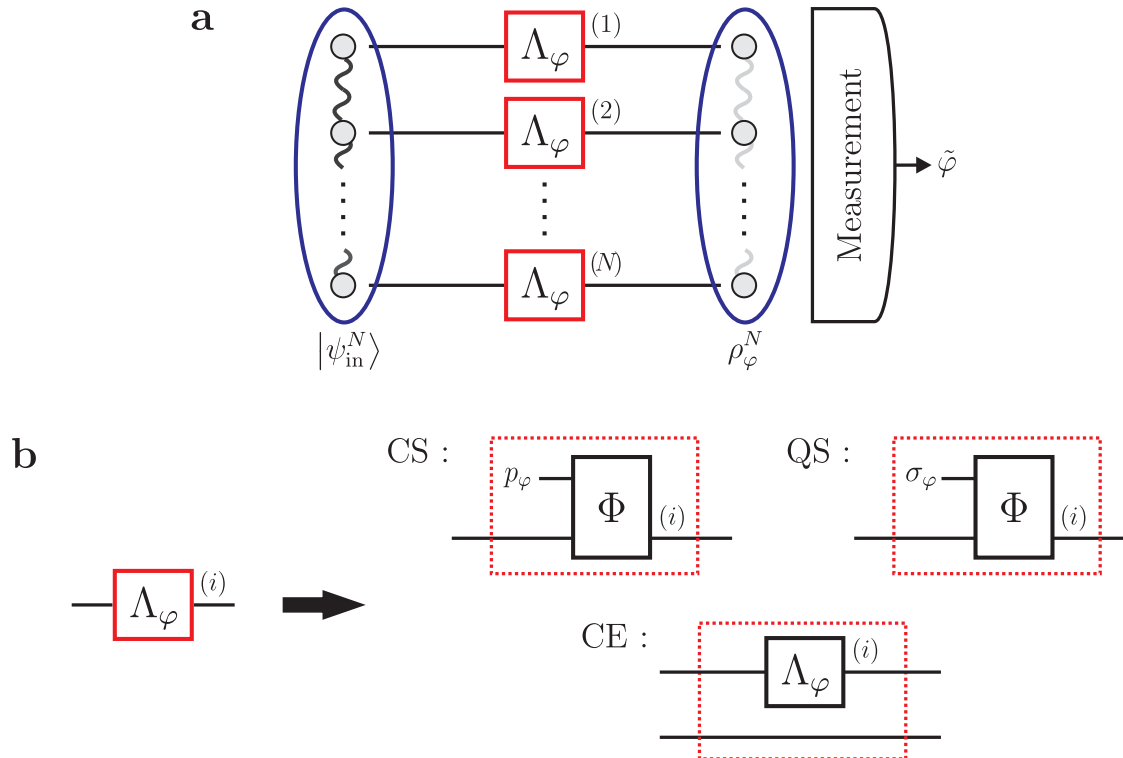


**Figure 1. Quantum metrology and the single channel methods**

(a) General scheme for quantum-enhanced metrology with uncorrelated noise. The  $N$  particles within the probe in a quantum state  $|\psi_{\text{in}}^N\rangle$  evolve and decohere independently while sensing an unknown parameter  $\varphi$  (e.g. phase). An estimate  $\tilde{\varphi}$  of the parameter is inferred from a measurement result on the final state of the probe  $\rho_{\varphi}^N$ .

(b) Precision bounds from single channel analysis. The ultimate precision is bounded by the  $1/\sqrt{N}$  scaling (SQL), if for small variations  $\delta\varphi$  around  $\varphi$  the channel  $\Lambda_{\varphi}$  can be expressed as a parameter-independent map  $\Phi$  that is also fed a classical, diagonal state  $p_{\varphi}$  – CS, or a general, quantum state  $\sigma_{\varphi}$  – QS, varying smoothly with  $\varphi$ . Still, for all such channels and more, the tightest bound on precision is obtained by the CE method, in which the map  $\Lambda_{\varphi}$  is replaced by its extension  $\Lambda_{\varphi} \otimes \mathcal{I}$ .

factor bound on the maximal quantum enhancement will force the asymptotic precision scaling to be SQL-like.

In this paper, we provide new insight into relations between seemingly unrelated methods used for derivations of various quantum metrological bounds and order them with respect to their predictive power. Firstly, focussing on the geometric intuitive method of channel *classical simulation* (CS) introduced in [36, 39], we prove that its applicability is equivalent to the approach proposed in [37]. Moreover, we show that the criterion for classical simulability of a channel can be generalized to a *quantum simulation* (QS) condition [36], which coincides with the channel programmability postulate of [34]. Although the idea of QS allows to prove the asymptotic SQL-like behaviour for a wider range of decoherence models, we demonstrate that the *channel extension* (CE) method of [39] encompasses all CS, [37], QS and [34] approaches providing more stringent bounds on precision. We also comment on the problem of

the tightness of these bounds, as they are guaranteed to be saturable only for channels, for which the estimation task cannot be improved by allowing for an additional ancilla (extension, idler mode) entangled with the input state. Classification of such channels is an open problem of current research both in channel estimation [41–44] and channel discrimination [45–53] theory. The graphical interpretation of the CS, QS and CE methods is presented in Figure 1b.

Most importantly, we go beyond the results of [39] and show that the CE method may be applied not only in the asymptotic regime but also when dealing with finite probes of  $N$  particles. Similarly to the asymptotic case, it corresponds then to an optimisation procedure over Kraus representations of a given channel that can be recast into an efficiently solvable semi-definite programming task. We apply our results to phase/frequency estimation with various noise models including: dephasing, depolarization, loss and spontaneous emission, restricting ourselves to the cases of noise commuting with the parameterized unitary part of the evolution. This assumption makes the analysis more transparent, but is not indispensable, since our methods may be effectively employed for any single particle evolution described by a general Lindblad equation [54] reshaped into the corresponding Kraus representation [55]. What is more, as our finite- $N$  CE method applies to models for which its asymptotic version fails, it can be used to upper-bound the asymptotic scaling for channels surpassing the SQL. As an example, in [40], our new method has been already utilized to predict asymptotic super-classical scaling for a channel with a non-commutative noise. Additionally, in order to stress the generality of the methods, in the final section of this paper we show that they can be applied not only to noisy unitary parameter estimation tasks but also to ones in which the decoherence strength itself is estimated. Finally, we should also clarify that noise correlation and memory effects [26, 56–58] are beyond the scope of this paper; while the non-Markovian effects, provided they affect each of the particles independently, might be analyzed using the tools presented, correlations between the decoherence processes affecting the particles does not fit well into the framework advocated here.

This paper is organised as follows. In Section 2 we introduce the mathematical tools of estimation theory designed to quantify the achievable precision in metrological schemes and discuss their applicability in the quantum setting. In Section 3 we study how these concepts may be utilized when the estimated parameter is encoded during the evolution of a given quantum system. Section 4 is devoted to quantum systems that consist of  $N$  particles undergoing independent evolution and contains the main results of the paper—methods allowing to quantify the ultimate precision both in the finite- $N$  and asymptotic  $N$  regimes as well as their direct application to phase estimation schemes. In Section 5 we show how these methods should be accommodated in order to encompass the frequency estimation tasks of atomic spectroscopy, whereas in Section 6 when considering metrological scenarios in which the strength of noise or loss is the parameter to be estimated. Section 7 contains additional discussion on consequences of the results obtained as well as an outlook on future research. Section 8 summarizes the

paper.

## 2. Quantum Fisher Information

### 2.1. Classical Cramér-Rao bound

Let us assume that after measuring a physical system an outcome is obtained that can be represented by a random variable  $X$  distributed with some probability distribution  $p_\varphi(X)$ . If the system is classically described, all its properties can be simultaneously determined, so that  $X$  can in principle be multidimensional and contain as much information about the system as allowed by the available resources. The estimation task corresponds then to determining with highest precision the quantity  $\varphi$  based on the observed value of  $X$ . As stated by the *Cramér-Rao bound* [59] any unbiased strategy to determine the unknown parameter after repeating the procedure  $k$  times, must provide an estimate  $\tilde{\varphi}$  with uncertainty that is lower bounded by

$$\Delta\tilde{\varphi} \geq \frac{1}{\sqrt{k F_{\text{cl}}[p_\varphi]}}, \quad \text{where} \quad F_{\text{cl}}[p_\varphi] = \int dx \frac{\dot{p}_\varphi(x)^2}{p_\varphi(x)} \quad (1)$$

is the (*classical*) *Fisher Information* (FI) ‡.

The  $1/\sqrt{k}$  dependence in (1) is a consequence of the central limit theorem and the fact that the  $k$  procedures are independent. This manifests itself by the additivity property of the FI, i.e.  $F_{\text{cl}}[p_\varphi^k] = k F_{\text{cl}}[p_\varphi]$  for  $X^k$ . Equation (1) shows that the FI is a *local* quantity containing information about infinitesimal variations of  $\varphi$ . That is why, FI is designed to be used in the so called *local estimation* approach in which small parameter fluctuations are to be sensed. This small deviations regime may always be reached after many procedure repetitions ( $k \rightarrow \infty$ ) and in this limit the Cramér-Rao bound is known to be saturable via e.g. max-likelihood estimation schemes [59].

### 2.2. Quantum Cramér-Rao bound

In a quantum estimation scenario, the parameter  $\varphi$  is encoded in a quantum state  $\rho_\varphi$ . A general measurement, mathematically represented by the elements of the *positive operator valued measure* (POVMs)  $M_x$  that satisfy  $M_x \geq 0$ ,  $\int dx M_x = \mathbb{I}$  § [60, 61], is performed yielding outcome statistics  $p_\varphi(X) = \text{Tr}\{\rho_\varphi M_X\}$ . Establishing the optimal estimation strategy corresponds then not only to the correct interpretation of the measurement results, but also to a non-trivial optimization over the class of all POVMs to find the measurement scheme maximizing the precision. In this case the *quantum Cramér-Rao bound* can be derived [62–64], which is independent of the choice of the POVMs and solely determined by the dependence of the output state on the estimated

‡ Throughout the paper, we depict derivatives w.r.t. the estimated parameter with an ‘overdot’, so that e.g.  $\dot{p}_\varphi(x) \equiv \partial_\varphi p_\varphi(x)$ ,  $\dot{\rho}_\varphi \equiv \partial_\varphi \rho_\varphi$  and  $\dot{K}(\varphi) \equiv \partial_\varphi K(\varphi)$ .

§ We denote by  $\mathbb{I}$ —the identity operator and by  $\mathcal{I}$ —the identity superoperator.

parameter:

$$\Delta\tilde{\varphi} \geq \frac{1}{\sqrt{k F_Q[\rho_\varphi]}} \quad \text{with} \quad F_Q[\rho_\varphi] = \text{Tr} \left\{ \rho_\varphi L^S[\rho_\varphi]^2 \right\} \quad (2)$$

being now the *quantum Fisher information* (QFI). The Hermitian operator  $L^S[\rho_\varphi]$  is the so called *symmetric logarithmic derivative* (SLD), which can be unambiguously defined for any state  $\rho_\varphi$  via the relation  $\dot{\rho}_\varphi = \frac{1}{2} (\rho_\varphi L^S[\rho_\varphi] + L^S[\rho_\varphi] \rho_\varphi)$ . Then, in the eigenbasis of  $\rho_\varphi = \sum_i \lambda_i(\varphi) |e_i(\varphi)\rangle\langle e_i(\varphi)|$  with  $\{|e_i(\varphi)\rangle\}_i$  forming a complete basis ( $\forall_i: 0 \leq \lambda_i \leq 1$ )

$$L^S[\rho_\varphi] = \sum_{i,j} \frac{2 \langle e_i(\varphi) | \dot{\rho}_\varphi | e_j(\varphi) \rangle}{\lambda_i(\varphi) + \lambda_j(\varphi)} |e_i(\varphi)\rangle\langle e_j(\varphi)|, \quad (3)$$

where the sum is taken over the terms with non-vanishing denominator. QFI is an additive quantity on product states and in particular  $F_Q[\rho_\varphi^{\otimes k}] = k F_Q[\rho_\varphi]$ . Thus, the  $\sqrt{k}$  term in the denominator of (2) may be equivalently interpreted as the number of independent repetitions of an experiment with a state  $\rho_\varphi$  or a single shot experiment with a multi-party state  $\rho_\varphi^{\otimes k}$ . Crucially, as proven in [64, 65], there always exist a measurement strategy, e.g. projection measurement in the eigenbasis of the SLD, for which bounds (1) and (2) coincide. Hence, as in the classical case, the saturability of (2) is guaranteed, but again only in the  $k \rightarrow \infty$  limit.

### 2.3. Purification-based definition of QFI

For pure states,  $\rho_\varphi = |\psi_\varphi\rangle\langle\psi_\varphi|$ , the QFI in (2) simplifies to  $F_Q[|\psi_\varphi\rangle] = 4 \left( \langle \dot{\psi}_\varphi | \dot{\psi}_\varphi \rangle - \left| \langle \dot{\psi}_\varphi | \psi_\varphi \rangle \right|^2 \right) \parallel$ . Yet, as indicated by (3), for general mixed states the computation of QFI involves diagonalisation of  $\rho_\varphi$ , which may be infeasible when dealing with large systems. That is why it is often necessary to look for upper bounds on QFI that would be efficiently calculable even at the expense of saturability. For this purpose, definitions of QFI were proposed that do not involve computing the SLD, but are specified at the level of state purifications:  $\rho_\varphi = \text{Tr}_E \{ |\Psi(\varphi)\rangle\langle\Psi(\varphi)| \}$ . In [38] the QFI of any  $\rho_\varphi$  has been proven to be equal to the smallest QFI of its purifications  $|\Psi(\varphi)\rangle \blacktriangleleft$ :

$$F_Q[\rho_\varphi] = \min_{\Psi(\varphi)} F_Q[|\Psi(\varphi)\rangle] = 4 \min_{\Psi(\varphi)} \left\{ \langle \dot{\Psi}(\varphi) | \dot{\Psi}(\varphi) \rangle - \left| \langle \dot{\Psi}(\varphi) | \Psi(\varphi) \rangle \right|^2 \right\}. \quad (4)$$

Independently, in [35] another purification-based QFI definition has been constructed:

$$F_Q[\rho_\varphi] = 4 \min_{\Psi(\varphi)} \langle \dot{\Psi}(\varphi) | \dot{\Psi}(\varphi) \rangle. \quad (5)$$

Despite apparent difference, Eqs. (4) and (5) are equivalent and one can prove that any purification minimizing one of them is likewise optimal for the other and satisfies the condition  $|\dot{\Psi}(\varphi)\rangle = \frac{1}{2} L^S[\rho_\varphi] \otimes \mathbb{I}_E |\Psi(\varphi)\rangle$  causing the second term of (4) to vanish.

$\parallel$  We shorten the notation of functions and superoperators of pure states, so that  $F[|\psi\rangle] \equiv F[|\psi\rangle\langle\psi|]$  and  $\Lambda[|\psi\rangle] \equiv \Lambda[|\psi\rangle\langle\psi|]$ .

$\blacktriangleleft$  See also an alternative formulation based on the convex roof formula, which is valid for unitary parameter estimation [66, 67].



Although for any suboptimal  $\Psi(\varphi)$  (4) must provide a strictly tighter bound on QFI than (5), the latter definition, owing to its elegant form, allows for more agility in the minimization procedure, so that it has been efficiently utilized in [35, 39] and is also the base for this paper.

#### 2.4. Right logarithmic derivative (RLD)-based upper bound on QFI

On the other hand, a natural way to construct a bound on QFI and avoid the SLD computation is to relax the Hermiticity condition of the logarithmic derivative. If a non-Hermitian  $L[\rho_\varphi]$  satisfying  $\partial_\varphi \rho_\varphi = \frac{1}{2} (\rho_\varphi L[\rho_\varphi] + L[\rho_\varphi]^\dagger \rho_\varphi)$  can be found, as proven in [63, 65], an upper limit on QFI in (2) is obtained:  $F_Q[\rho_\varphi] \leq \text{Tr}\{\rho_\varphi L[\rho_\varphi] L[\rho_\varphi]^\dagger\}$ . In particular, if and only if  $\partial_\varphi \rho_\varphi$  is contained within the support of  $\rho_\varphi$ , one can construct the *Right Logarithmic Derivative* (RLD) by setting  $L[\rho_\varphi] = L^R[\rho_\varphi] = \rho_\varphi^{-1} \partial_\varphi \rho_\varphi$  and formulate an upper bound on QFI of a simpler form:

$$F_Q[\rho_\varphi] \leq F_Q^{\text{RLD}}[\rho_\varphi] = \text{Tr}\{\rho_\varphi^{-1} (\partial_\varphi \rho_\varphi)^2\}. \quad (6)$$

Although (6) is tight only when  $L^R[\rho_\varphi] = L^S[\rho_\varphi]$ , it still allows one to quantify precision well for channel estimation tasks [37], as described in the following section. Lastly, one should note that we are not considering here multi-parameter estimation schemes, for which the RLD may sometimes provide tighter bounds than the SLD [68, 69].

### 3. Estimation of a quantum channel

#### 3.1. Channel QFI

As in metrological setups the estimated parameter is encoded in the evolution of a system, we identify  $\rho_\varphi = \Lambda_\varphi[\rho_{\text{in}}]$  as the final state of a system that started from an input  $\rho_{\text{in}}$ . The preparation of  $\rho_{\text{in}}$  is controlled in order to achieve the most precise estimate of  $\varphi$  that parametrizes some general *channel*—a *Completely Positive Trace Preserving* (CPTP) map  $\Lambda_\varphi$  [60, 61]. Although the form of  $\Lambda_\varphi$  in general strongly depends on the model considered, the Quantum Cramér-Rao bound always applies, so that precision is upper bounded according to (2) with QFI  $F_Q[\Lambda_\varphi[\rho_{\text{in}}]]$ . Furthermore, as the QFI is a convex quantity [70], one should restrict oneself to pure input states when seeking the optimal one. Hence, as shown in Figure 2a, we define the *channel QFI* as the maximal QFI after performing the input optimisation, so that it has a concrete operational and application-like interpretation

$$\mathcal{F}[\Lambda_\varphi] = \max_{\psi_{\text{in}}} F_Q[\Lambda_\varphi[|\psi_{\text{in}}\rangle]]. \quad (7)$$

For instance, while estimating the duration of the evolution ( $\varphi \equiv t$ ) in an ideal, decoherence-free setting, the CPTP map is unitary leading to a pure channel output. Thus,  $\Lambda_\varphi[|\psi_{\text{in}}\rangle] = \mathcal{U}_t[|\psi_{\text{in}}\rangle] = e^{-iHt} |\psi_{\text{in}}\rangle \langle \psi_{\text{in}}| e^{iHt}$  with  $H$  being the Hamiltonian of the evolution. Hence, the definition (7) corresponds to

$$\mathcal{F}[\mathcal{U}_t] = \max_{\psi_{\text{in}}} F_Q[e^{-iHt} |\psi_{\text{in}}\rangle] = 4 \max_{\psi_{\text{in}}} \{ \langle \psi_{\text{in}} | H^2 | \psi_{\text{in}} \rangle - \langle \psi_{\text{in}} | H | \psi_{\text{in}} \rangle^2 \} = 4 \max_{\psi_{\text{in}}} \Delta^2 H, \quad (8)$$

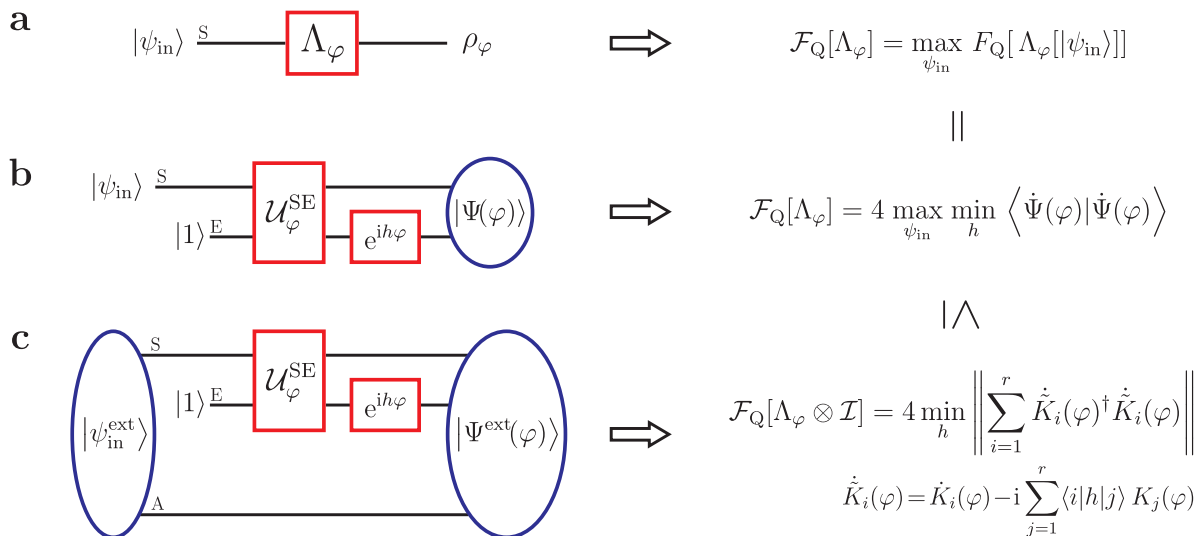


**Figure 2. Channel QFI based on the output state purification**

- (a) Channel QFI as the QFI of the output state maximized over all pure input states.  
 (b) Channel QFI obtained from the output state purification generated by a local, fictitious, parameter-dependent environment rotation.  
 (c) Extended channel QFI independent of the maximization over the input states. The environment rotation corresponds to a choice of Kraus representation of the channel.

and the optimal states are the ones that maximize the Hamiltonian variance. Note also that in this case the quantum Cramér-Rao bound takes the form of the time-energy uncertainty relation,  $\Delta H \cdot \Delta \tilde{t} \geq 1/2$  [71, 72], with  $\Delta \tilde{t}$  being the uncertainty in the estimated duration.

### 3.2. Purification-based definition of channel QFI

In order to employ the definition (5), we utilize the Stinespring theorem [61] and express the channel  $\Lambda_\varphi$  as a unitary map  $U_\varphi^{\text{SE}}$  on the system combined with an environment disregarded after the evolution. In this way, the output state and its purification respectively read  $\Lambda_\varphi[|\psi_{\text{in}}\rangle] = \text{Tr}_E\{|\Psi(\varphi)\rangle\langle\Psi(\varphi)|\}$  and  $|\Psi(\varphi)\rangle = U_\varphi^{\text{SE}} |\psi_{\text{in}}\rangle \otimes |1\rangle$ , where  $|1\rangle$  is an arbitrary fixed state chosen to be the first vector in the basis  $\{|i\rangle\}_{i=1}^r$  of the environment Hilbert space  $\mathcal{H}_E^r$ . By specifying the dimension  $r$  of  $\mathcal{H}_E^r$  to be equal to the rank of  $\Lambda_\varphi$ , we can generate all non-trivial purifications,  $\tilde{\Psi}(\varphi)$ , by applying a fictitious, possibly  $\varphi$ -dependent unitary rotation,  $u_\varphi^E$ , to the environment, so that  $|\tilde{\Psi}(\varphi)\rangle = \tilde{U}_\varphi^{\text{SE}} |\psi_{\text{in}}\rangle \otimes |1\rangle$  with  $\tilde{U}_\varphi^{\text{SE}} = u_\varphi^E U_\varphi^{\text{SE}}$ . Furthermore, writing the channel action in its Kraus representation form  $\Lambda_\varphi[|\psi_{\text{in}}\rangle] = \sum_{i=1}^r \tilde{K}_i(\varphi) |\psi_{\text{in}}\rangle\langle\psi_{\text{in}}| \tilde{K}_i(\varphi)^\dagger$ , we can identify the Kraus operators corresponding to  $\tilde{\Psi}(\varphi)$  as

$$\tilde{K}_i(\varphi) = \langle i | \tilde{U}_\varphi^{\text{SE}} | 1 \rangle = \sum_{j=1}^r u_{\varphi,ij}^E K_j(\varphi), \quad (9)$$

where  $u_{\varphi,ij}^E = \langle i | u_\varphi^E | j \rangle$  and  $K_j(\varphi) = \langle j | U_\varphi^{\text{SE}} | 1 \rangle$  are the Kraus operators of the original purification  $\Psi(\varphi)$ . Hence, by picking an environment unitary rotation  $u_\varphi^E$ ,

we are, equivalently to the purification choice, specifying a Kraus representation of  $\Lambda_\varphi$ . Moreover, as the QFI is a local quantity, we can restrict ourselves to infinitesimal rotations,  $u_\varphi^E = e^{-ih(\varphi - \varphi_0)}$ , in the vicinity of the real value  $\varphi_0$  that are generated by some Hermitian  $h$ . Taking without loss of generality  $\varphi_0 = 0$ , we obtain the channel version of (5) shown in Figure 2b as

$$\mathcal{F}[\Lambda_\varphi] = 4 \max_{\psi_{\text{in}}} \min_h \langle \dot{\tilde{\Psi}}(\varphi) | \dot{\tilde{\Psi}}(\varphi) \rangle = 4 \max_{\psi_{\text{in}}} \min_h \langle \psi_{\text{in}} | \sum_{i=1}^r \dot{K}_i(\varphi)^\dagger \dot{K}_i(\varphi) | \psi_{\text{in}} \rangle, \quad (10)$$

where  $|\dot{\tilde{\Psi}}(\varphi)\rangle = (\dot{U}_\varphi^{\text{SE}} - ihU_\varphi^{\text{SE}})|\psi_{\text{in}}\rangle \otimes |1\rangle$  and similarly  $\dot{K}_i(\varphi) = \dot{K}_i(\varphi) - i \sum_{j=1}^r h_{ij} K_j(\varphi)$  with  $h_{ij} = \langle i | h | j \rangle$  being the elements of the generator of Kraus representation rotations (9). Crucially, Figure 2b and Equation (10) indicate that the optimal purification/Kraus representation corresponds to the choice of an artificial environment that rotates locally with  $\varphi$  hindering as much as possible information about the estimated parameter.

In order to make the reader familiar with the above formalism, we apply the definition (10) to the previously mentioned case of the evolution duration estimation  $\mathcal{U}_t[|\psi_{\text{in}}\rangle]$ . As the evolution is unitary and  $r = 1$ , the environment/Kraus rotations correspond just to a phase variation  $u_t^E = e^{-iht}$  with  $h$  being a real scalar. Hence, (10) simplifies to (8) as expected:

$$\mathcal{F}[\mathcal{U}_t] = 4 \max_{\psi_{\text{in}}} \min_h \{ \langle \psi_{\text{in}} | H^2 | \psi_{\text{in}} \rangle - 2h \langle \psi_{\text{in}} | H | \psi_{\text{in}} \rangle + h^2 \} = 4 \max_{\psi_{\text{in}}} \Delta^2 H \quad (11)$$

with minimum occurring at  $h = \langle \psi_{\text{in}} | H | \psi_{\text{in}} \rangle$ . Consistently, we would also arrive at (8), if we had used the other QFI purification-based definition (4) as shown in [38].

### 3.3. Extended channel QFI

The channel QFI (7) is affected by any  $\varphi$ -variations in the form of  $\Lambda_\varphi$ , quantifying the distinguishability between maps  $\Lambda_\varphi$  and  $\Lambda_{\varphi + \delta\varphi}$ . However, any such disturbance may be noticeable only for input states which lead to a measurable change of the channel output that is at best in some ‘‘orthogonal direction’’. As a consequence, the quantity  $\min_h \{ \dots \}$  in (10) depends strongly on the pure input  $\psi_{\text{in}}$ , as the minimum occurs for Kraus operators  $\{K_i^{\text{opt}}(\varphi)\}_{i=1}^r$  which fulfill the condition  $\dot{K}_i^{\text{opt}}(\varphi) |\psi_{\text{in}}\rangle = \frac{1}{2} L^S[\Lambda_\varphi[|\psi_{\text{in}}\rangle]] K_i^{\text{opt}}(\varphi) |\psi_{\text{in}}\rangle$  required for the purification of (4) and (5) to be optimal. Maximization of this quantity over  $|\psi_{\text{in}}\rangle$  is difficult in general, due to the impossibility of exchanging the order of max and min in (10) [35].

Yet, one may construct a natural upper bound on the channel QFI (7) by *extending* the input space,  $\mathcal{H}_S$ , by an equally-large auxiliary space,  $\mathcal{H}_A$ , which is unaffected by the map and measured along with the channel output (see Figure 2c). This way, by employing extended input states entangled between these two spaces,  $|\psi_{\text{in}}^{\text{ext}}\rangle \in \mathcal{H}_S \times \mathcal{H}_A$ , one may acquire full available information about  $\varphi$  imprinted by the map  $\Lambda_\varphi$  on the extended output state. The analogue of (10) defines then the *extended channel QFI* [35]:

$$\mathcal{F}[\Lambda_\varphi \otimes \mathcal{I}] = 4 \max_{\rho_{\text{in}}^S} \min_h \text{Tr}_S \left\{ \rho_{\text{in}}^S \sum_{i=1}^r \dot{K}_i(\varphi)^\dagger \dot{K}_i(\varphi) \right\} = 4 \min_h \left\| \sum_{i=1}^r \dot{K}_i(\varphi)^\dagger \dot{K}_i(\varphi) \right\|, \quad (12)$$

where  $\|\dots\|$  represents the operator norm. The first expression is obtained by tracing over the auxiliary space  $\mathcal{H}_A$ , what leads to the maximisation over all mixed states  $\rho_{\text{in}}^S = \text{Tr}_A\{|\psi_{\text{in}}^{\text{ext}}\rangle\langle\psi_{\text{in}}^{\text{ext}}|\}$ . However, this is exactly (10) with the pure input state replaced by a general mixed one, in which case the order of max and min can be swapped [35]<sup>+</sup>. Consistently, if the optimal input state of (12) is pure, (10) and (12) become equivalent manifesting the uselessness of entanglement between  $\mathcal{H}_S$  and  $\mathcal{H}_A$  and the irrelevance of the auxiliary space.

Importantly, the extended channel QFI (12) can always be efficiently evaluated numerically by means of semi-definite programming [39] and we show that this is a special case of a more general task of bounding  $N$ -parallel channels QFI, as explained in Appendix E. For phase estimation schemes with relevant noise models including: *dephasing*, *depolarization*, *loss* and *spontaneous emission*, we determine analytically both (10) and (12) to verify if the use of extended, entangled input states may improve estimation at the single channel level. The corresponding unextended/extended channel QFIs are presented in Table 1, whereas the optimal purifications yielding the minimum of (12) can be found in Appendix A along with the details of the channels considered. The results justify that extension enhances the precision only for depolarization and spontaneous emission channels, for which the input states maximally entangled between  $\mathcal{H}_S$  and  $\mathcal{H}_A$  are optimal.

### 3.4. RLD-based upper bound on extended channel QFI

In [37] the applicability of the RLD-based bound (6) has been addressed in the context of channels. By defining the *Choi-Jamiołkowski* (C-J) *representation* [61] of a particular map  $\Lambda_\varphi$  as  $\Omega_{\Lambda_\varphi} = \Lambda_\varphi \otimes \mathcal{I} [|\mathbb{I}\rangle]$  with  $|\mathbb{I}\rangle = \sum_{i=1}^{\dim \mathcal{H}_S} |i\rangle \otimes |i\rangle$ , it has been proven that the extended channel QFI can be further upper-bounded by

$$\mathcal{F}[\Lambda_\varphi \otimes \mathcal{I}] \leq \mathcal{F}^{\text{RLD}}[\Lambda_\varphi \otimes \mathcal{I}] = \left\| \text{Tr}_{\mathcal{A}} \left\{ \dot{\Omega}_{\Lambda_\varphi} \Omega_{\Lambda_\varphi}^{-1} \dot{\Omega}_{\Lambda_\varphi} \right\} \right\|, \quad (13)$$

where  $\|\dots\|$  is again the operator norm and  $\Omega_{\Lambda_\varphi}^{-1}$  is the inverse of  $\Omega_{\Lambda_\varphi}$  restricted only to the support of the C-J matrix. Most importantly, the bound (13) is determined solely by the form of  $\Lambda_\varphi$ , i.e. its C-J representation, and does not contain any extra information about the space of input states accepted by the map. This contrasts the definitions of purification-based unextended/extended channel QFIs (10)/(12) and facilitates the analyticity of the results presented in Table 1. On the other hand, as indicated in Section 2.4, both applicability and tightness of the RLD-based bounds are limited. The bound (13) is valid only when  $\dot{\Omega}_{\Lambda_\varphi}^2$  is fully supported by  $\Omega_{\Lambda_\varphi}$  [37]. However, we give an intuitive reason for this restriction by proving that this condition is equivalent (see Appendix B) to the notion of channel  $\Lambda_\varphi$  being  $\varphi$ -*non-extremal*, as introduced in [39] and also revisited in the following section. This confirms that the exclusive dependence of (13) on  $\Omega_{\Lambda_\varphi}$  has indeed a strong geometrical meaning. Moreover, although the RLD-based bounds depicted in Table 1 for the relevant channels seem to be far above the

<sup>+</sup> We should stress that (12) *does not* correspond to the situation of using *mixed* states as inputs for *unextended* channel, as mixed states never outperform pure state inputs due to convexity of the QFI.

Noise model	$\mathcal{F}[\Lambda_\varphi]$	$\mathcal{F}[\Lambda_\varphi \otimes \mathcal{I}]$	$\mathcal{F}_{\text{as}}^{\text{CE}}$ in [39]	$\mathcal{F}_{\text{as}}^{\text{QS}}$	$\mathcal{F}^{\text{RLD}}[\Lambda_\varphi \otimes \mathcal{I}]$	$\mathcal{F}_{\text{as}}^{\text{CS}}$ in [39]
<i>Dephasing</i>	$\eta^2$	$\eta^2$	$\frac{\eta^2}{1-\eta^2}$	$\frac{\eta^2}{1-\eta^2}$	$\frac{\eta^2}{1-\eta^2}$	$\frac{\eta^2}{1-\eta^2}$
<i>Depolarization</i>	$\eta^2$	$\frac{2\eta^2}{1+\eta}$	$\frac{2\eta^2}{(1-\eta)(1+2\eta)}$	$\frac{2\eta^2}{(1-\eta)(1+2\eta)}$	$\frac{2\eta^2(1+\eta)}{(1-\eta)(1+3\eta)}$	$\frac{4\eta^2}{(1-\eta)(1+3\eta)}$
<i>Loss</i>	$\eta$	$\eta$	$\frac{\eta}{1-\eta}$	$\frac{\eta}{1-\eta}$	n.a.	n.a.
<i>Spontaneous emission</i>	$\eta$	$\frac{4\eta}{(1+\sqrt{\eta})^2}$	$\frac{4\eta}{1-\eta}$	n.a.	n.a.	n.a.

**Table 1. Channel phase estimation sensitivity quantified via QFIs and their asymptotic bounds.** The noise models of metrological relevance discussed in the paper are listed in the first column. Decoherence strength increases with a decrease of the  $\eta$  parameter ( $0 \leq \eta < 1$ ) (see Appendix A for details). From left to right—single channel QFI, extended channel QFI, upper bounds on asymptotic channel QFI (16) in ascending order: CE bound (see Section 4.1.3), QS bound (see Section 4.1.2), RLD-based bound (see Section 3.4), CS bound (see Section 4.1.1). [n.a.—not available]

corresponding channel QFIs—(7) and (12), they are of great significance. The bound (13) is additive for any maps  $\Lambda_\varphi^{(1)}, \Lambda_\varphi^{(2)}$  to which it applies [37], thus

$$\begin{aligned} \mathcal{F}^{\text{RLD}}[(\Lambda_\varphi^{(1)} \otimes \mathcal{I}) \otimes (\Lambda_\varphi^{(2)} \otimes \mathcal{I})] &= \mathcal{F}^{\text{RLD}}[\Lambda_\varphi^{(1)} \otimes \mathcal{I}] + \mathcal{F}^{\text{RLD}}[\Lambda_\varphi^{(2)} \otimes \mathcal{I}] \\ \therefore \mathcal{F}[(\Lambda_\varphi \otimes \mathcal{I})^{\otimes N}] &\leq \mathcal{F}^{\text{RLD}}[(\Lambda_\varphi \otimes \mathcal{I})^{\otimes N}] = N \mathcal{F}^{\text{RLD}}[\Lambda_\varphi \otimes \mathcal{I}]. \end{aligned} \quad (14)$$

Hence, it constrains not only the QFI of a single extended channel, but also restricts the QFI of  $N$  extended channels used in parallel to scale at most linearly with  $N$ . Crucially, as the extension can only improve the precision, (14) is also a valid upper-bound on the QFI of  $N$  uses of an unextended channel, which asymptotic precision scaling is then limited to a constant factor improvement over the SQL (see Section 4.1).

#### 4. Estimation of $N$ independent quantum channels

In order to describe general metrological schemes depicted in Figure 1a, we model the evolution of all particles within the probe as  $N$  identical, independent channels acting on a possibly entangled, pure input state of the whole probe  $|\psi_{\text{in}}^N\rangle$ . The final output state of the probe then reads  $\rho_\varphi^N = \Lambda_\varphi^{\otimes N} [|\psi_{\text{in}}^N\rangle]$  yielding the  $N$ -channel QFI:

$$\mathcal{F}[\Lambda_\varphi^{\otimes N}] = \max_{\psi_{\text{in}}^N} F_{\text{Q}}[\Lambda_\varphi^{\otimes N} [|\psi_{\text{in}}^N\rangle]], \quad (15)$$

which linear or quadratic dependence on  $N$  dictates respectively the SQL or HL scaling of precision. For example, when considering classical schemes that employ unentangled probes,  $|\psi_{\text{in}}^N\rangle = \otimes_{n=1}^N |\psi_{\text{in}}^1\rangle$ , we are effectively dealing with  $N$  independent subsystems, so that  $\mathcal{F}[\Lambda_\varphi^{\otimes N}] = N \mathcal{F}[\Lambda_\varphi]$  and the uncertainty of the estimate  $\tilde{\varphi}$  decreases as  $1/\sqrt{N}$ .

#### 4.1. Standard quantum limit (SQL)-like bounds on precision in the asymptotic $N$ limit

To investigate channels that incorporate the uncorrelated noise restricting the asymptotic precision scaling to SQL, we define the *asymptotic channel QFI* as

$$\mathcal{F}_{\text{as}}[\Lambda_\varphi] = \lim_{N \rightarrow \infty} \frac{\mathcal{F}[\Lambda_\varphi^{\otimes N}]}{N}. \quad (16)$$

Thus, for such SQL-bound channels, (16) is finite and  $\mathcal{F}_{\text{as}}[\Lambda_\varphi] \geq \mathcal{F}[\Lambda_\varphi]$  with equality indicating the optimality of classical estimation schemes. Hence, (16) quantifies the *maximal quantum precision enhancement* that reads

$$\chi[\Lambda_\varphi] = \lim_{N \rightarrow \infty} \frac{\Delta\tilde{\varphi}_{\text{cl}}}{\Delta\tilde{\varphi}_{\text{Q}}} = \sqrt{\frac{\mathcal{F}_{\text{as}}[\Lambda_\varphi]}{\mathcal{F}[\Lambda_\varphi]}} \geq 1. \quad (17)$$

However, as the computation of (16) is generally infeasible owing to the complexity of QFI rising exponentially with  $N$ , one normally needs to construct an upper limit on the  $N$ -channel QFI (15),  $\mathcal{F}^{\text{bound}}[\Lambda_\varphi^{\otimes N}]$ , from which the asymptotic form,  $\mathcal{F}_{\text{as}}^{\text{bound}}$ , may be deduced using (16) that upper-bounds both the  $N$ -channel QFI and the maximal quantum precision enhancement:

$$\mathcal{F}[\Lambda_\varphi^{\otimes N}] \leq N \mathcal{F}_{\text{as}}^{\text{bound}}, \quad \chi[\Lambda_\varphi] \leq \sqrt{\frac{\mathcal{F}_{\text{as}}^{\text{bound}}[\Lambda_\varphi]}{\mathcal{F}[\Lambda_\varphi]}}. \quad (18)$$

Methods of constructing  $\mathcal{F}_{\text{as}}^{\text{bound}}$  were proposed in [39] basing on the concepts of channel *classical simulation* (CS) and *channel extension* (CE). As mentioned already, the CS method applies only to  $\varphi$ -non-extremal channels, for which also the RLD-based bound (14) provides a valid example of  $\mathcal{F}_{\text{as}}^{\text{bound}}$ . Yet, the notion of CS may be generalized to the idea of channel *quantum simulation* (QS) introduced in [36], in order to obtain an asymptotic bound applicable to a wider class of quantum maps. All these four approaches ( $\mathcal{F}_{\text{as}}^{\text{bound}} = \mathcal{F}_{\text{as}}^{\text{CS}}, \mathcal{F}_{\text{as}}^{\text{CE}}, \mathcal{F}^{\text{RLD}}[\Lambda_\varphi \otimes \mathcal{I}], \mathcal{F}_{\text{as}}^{\text{QS}}$  respectively) are presented in Table 1 on the right hand side of the double-line for the relevant channels. As the lossy and spontaneous emission interferometry cases are examples of  $\varphi$ -extremal maps, they do not allow for finite  $\mathcal{F}_{\text{as}}^{\text{CS}}$  and  $\mathcal{F}^{\text{RLD}}[\Lambda_\varphi \otimes \mathcal{I}]$  to be constructed. In the case of depolarization channel, which is full-rank [61] and hence  $\varphi$ -non-extremal, despite the lack of a simple geometric interpretation of its value,  $\mathcal{F}^{\text{RLD}}[\Lambda_\varphi \otimes \mathcal{I}]$  proves to be tighter than  $\mathcal{F}_{\text{as}}^{\text{CS}}$ . The more general QS approach not only applies also to the ( $\varphi$ -extremal) lossy interferometry case, but also provides as accurate bounds as the CE method. Nevertheless, as the CE approach is proven to provide at least as tight bounds for the broadest class of quantum channels containing ones to which the other methods apply, we use it to quantify the maximal quantum precision enhancements (17) for the channels considered (see Table 2). Below, we describe alternately the CS, QS and CE methods—ordered according to their power and generality.



#### 4.1.1. Classical simulation (CS) method

As introduced in [36] and depicted in Figure 1b, a channel admits a CS of itself, if for any  $\varrho$  it is expressible in the form

$$\Lambda_\varphi[\varrho] = \Phi[\varrho \otimes p_\varphi] = \sum_i p_{\varphi,i} \Pi_i[\varrho], \quad (19)$$

where  $p_\varphi = \sum_i p_{\varphi,i} |e_i\rangle\langle e_i|$  is a classical, diagonal density matrix in some basis and  $\Phi$  is a  $\varphi$ -independent CPTP map acting on a larger input space. By defining  $\Pi_i[\varrho] = \Phi[\varrho \otimes |e_i\rangle\langle e_i|]$  one obtains the second equality in (19), so that it becomes evident that the estimated  $\varphi$  parametrizes only the mixing probabilities of some  $\varphi$ -independent quantum maps. Then, the  $N$ -channel QFI (15) can be simply upper-bounded via  $\mathcal{F}[\Lambda_\varphi^{\otimes N}] \leq N F_{\text{cl}}[p_{\varphi,i}]$ , where  $F_{\text{cl}}[p_{\varphi,i}]$  is the discrete version of classical FI in (1) and plays the role of  $\mathcal{F}_{\text{as}}^{\text{bound}}$  in (18) [36, 39]. Moreover, as QFI is a local quantity, in order to construct a CS-based  $\mathcal{F}_{\text{as}}^{\text{bound}}$  valid for small deviations  $\delta\varphi$  around a given  $\varphi$ , the classical simulation must be feasible only locally, i.e.  $\Lambda_\varphi[\varrho] = \sum_i p_{\varphi,i} \Pi_i[\varrho] + O(\delta\varphi^2)$ . Therefore, as proven in [36], if the C-J representation  $\Omega_{\Lambda_\varphi}$  of a channel  $\Lambda_\varphi$  allows for parameters  $\epsilon_\pm > 0$  such that the matrices  $\Omega_{\Pi_\pm} = \Omega_{\Lambda_\varphi} \pm \epsilon_\pm \dot{\Omega}_{\Lambda_\varphi}$  are positive semi-definite at a given  $\varphi$ , the channel is  $\varphi$ -non-extremal there and the necessary  $p_{\varphi,i}$  can always be found. This is because one can construct  $\Omega_{\tilde{\Lambda}_\varphi} = p_{\varphi,+} \Omega_{\Pi_+} + p_{\varphi,-} \Omega_{\Pi_-}$  that up to  $O(\delta\varphi^2)$  coincides with  $\Omega_{\Lambda_\varphi}$  by choosing  $p_{\varphi,\pm}$  such that  $\Omega_{\tilde{\Lambda}_\varphi} = \Omega_{\Lambda_\varphi}$  and  $\dot{\Omega}_{\tilde{\Lambda}_\varphi} = \dot{\Omega}_{\Lambda_\varphi}$ . Hence,  $\Lambda_\varphi[\varrho] = \tilde{\Lambda}_\varphi[\varrho] + O(\delta\varphi^2)$  with  $\tilde{\Lambda}_\varphi[\varrho] = p_{\varphi,+} \Pi_+ + p_{\varphi,-} \Pi_-$ , so that  $F_{\text{cl}}[p_{\varphi,\pm}] = 1/(\epsilon_+ \epsilon_-)$  is a legal example of the required finite bound valid at  $\varphi$ . Furthermore, in [39], it has been proven that for channels of the form  $\Lambda_\varphi[\varrho] = \Lambda[\mathcal{U}_\varphi[\varrho]]$  this two-point construction is always optimal at any  $\varphi$  when maximal possible  $\epsilon_\pm$  are chosen\*. Geometrically, imagining the convex set of all CPTP maps in their C-J representation that share input and output spaces of  $\Lambda_\varphi$ , the channels  $\Omega_{\Pi_\pm}$  lie at the intersection points of the tangent generated by  $\dot{\Omega}_{\Lambda_\varphi}$  at  $\Omega_{\Lambda_\varphi}$  and the boundary of the set. The  $\mathcal{F}_{\text{as}}^{\text{bound}}$  of (18), which we refer to as the *asymptotic CS bound*— $\mathcal{F}_{\text{as}}^{\text{CS}} = 1/(\epsilon_+^{\text{max}} \epsilon_-^{\text{max}})$ , is dictated then by the “distances”  $\epsilon_\pm^{\text{max}}$  of the channel to the boundary measured along this tangent. Although the CS approach provides weaker bounds than the CE method [39], it gives an intuitive geometric explanation of the inevitable asymptotic SQL-like scaling of all  $\varphi$ -non-extremal maps. These naturally include the full-rank channels [61], which lie inside the set of CPTP maps away from its boundary.

#### 4.1.2. Quantum simulation (QS) method

In [36], a natural generalization of the channel CS has been proposed which is schematically presented in Figure 1b. This, so called, QS of a channel corresponds to expressing its action in a form similar to (19) that reads

$$\Lambda_\varphi[\varrho] = \Phi[\varrho \otimes \sigma_\varphi] = \text{Tr}_{\mathbb{E}_\Phi \mathbb{E}_\sigma} \left\{ U \left( \varrho \otimes |\psi_\varphi\rangle_{\mathbb{E}_\Phi \mathbb{E}_\sigma} \langle \psi_\varphi| \right) U^\dagger \right\}, \quad (20)$$

where now  $\sigma_\varphi$  is a quantum, non-diagonal,  $\varphi$ -dependent density matrix, and the purified form on the right hand side involves both channel  $\Phi$  environment space  $\mathbb{E}_\Phi$  as well as

\* Yet, it may prove optimal for channels of other type, as shown for transversal dephasing in [40].

$\sigma_\varphi$  purification space  $E_\sigma$ , such that  $\sigma_\varphi = \text{Tr}_{E_\sigma}\{|\psi_\varphi\rangle\langle\psi_\varphi|\}$ . Note that the notion of *quantum simulability* is equivalent to the *channel programmability* concept introduced in [34]. Following the same argumentation as in [39] for CS, the  $N$ -channel QFI (15) of a *quantum simulable channel*—one admitting a QS of the form (20) with finite  $F_Q[\sigma_\varphi]$ —can be linearly bounded as  $\mathcal{F}[\Lambda_\varphi^{\otimes N}] \leq N F_Q[\sigma_\varphi]$ , and therefore the asymptotic bound reads  $\mathcal{F}_{\text{as}}^{\text{bound}} = F_Q[\sigma_\varphi]$ . Similarly to CS, a channel may admit many decompositions (20) and the optimal one must yield the lowest  $F_Q[\sigma_\varphi]$ . Therefore, without loss of generality, in the search for the optimal QS, we may take  $U$  in (20) to act on the full purified system, i.e. also in  $E_\Phi$  and  $E_\sigma$  spaces. This enlarges the set of all possible QSs beyond the original ones  $U = U^{\text{SE}_\Phi} \otimes \mathbb{I}^{E_\sigma}$  and yields  $\mathcal{F}_{\text{as}}^{\text{bound}} = F_Q[|\psi_\varphi\rangle]$ , which via (4) cannot be smaller than  $F_Q[\sigma_\varphi]$ . In fact, (4) assures that for any QS employing  $\sigma_\varphi$ , there exists an “enlarged” decomposition (20) leading to the same  $\mathcal{F}_{\text{as}}^{\text{bound}}$  with  $|\psi_\varphi\rangle$  being the minimal purification in (4). In conclusion, we may seek the optimal QS by analysing all possible decompositions of the form (20) that, owing to the locality of the QFI, must be feasible only for small deviations  $\delta\varphi$  from a given  $\varphi$ , so that  $\Lambda_\varphi[\varrho] = \text{Tr}_{E_\Phi E_\sigma}\{U(\varrho \otimes |\psi_\varphi\rangle\langle\psi_\varphi|)U^\dagger\} + O(\delta\varphi^2)$ . In Appendix D, we prove that, in order for the QS (20) to be possible locally at  $\varphi$  and lead to a finite asymptotic bound,  $\Lambda_\varphi$  of rank  $r$  must admit Kraus operators  $\{K_i(\varphi)\}_{i=1}^r$  that satisfy the two conditions:

$$i \sum_{i=1}^r \dot{K}_i(\varphi)^\dagger K_i(\varphi) = 0 \quad \text{and} \quad \sum_{i=1}^r \dot{K}_i(\varphi)^\dagger \dot{K}_i(\varphi) = \frac{1}{4} F_Q[|\psi_\varphi\rangle] \mathbb{I}. \quad (21)$$

Hence, by optimizing over all locally equivalent Kraus representations of  $\Lambda_\varphi$ —the ones related to one another by rotations (9) generated by any Hermitian  $h$ —that satisfy constraints (21), we may determine the asymptotic bound given by the optimal local QS, which we refer to as the *asymptotic QS bound*— $\mathcal{F}_{\text{as}}^{\text{QS}}$ , as follows

$$\mathcal{F}_{\text{as}}^{\text{QS}} = \min_h \lambda \quad \text{s.t.} \quad \alpha_{\tilde{K}} = \frac{\lambda}{4} \mathbb{I}, \quad \beta_{\tilde{K}} = 0, \quad (22)$$

where  $\alpha_{\tilde{K}} = \sum_{i=1}^r \dot{K}_i(\varphi)^\dagger \dot{K}_i(\varphi)$ ,  $\beta_{\tilde{K}} = i \sum_{i=1}^r \dot{K}_i(\varphi)^\dagger \tilde{K}_i(\varphi)$  and  $\lambda$  has the interpretation of  $\mathcal{F}_{\text{as}}^{\text{bound}} = F_Q[|\psi_\varphi\rangle]$  for a local QS of the form (20). Before revisiting the CE method explicitly below, we should note that (22) resembles exactly the asymptotic CE bound of [39] with an extra constraint forcing the operator  $\alpha_{\tilde{K}}$  to be proportional to identity. This proves that indeed the QS method can never outperform the CE approach.

Investigating the relevant quantum maps considered in Table 1, the QS method must naturally apply to dephasing and depolarization channels. These are  $\varphi$ -non-extremal maps, hence their locally constructible CSs (19) serve as examples of the more general QSs (20). Consistently, the Kraus representations utilized in [39] to obtain the asymptotic CE bounds for these two channels fulfil the  $\alpha_{\tilde{K}} \propto \mathbb{I}$  constraint. Thus, QS is not only feasible in their case but also its asymptotic bound coincides with the one of the superior CE method. Significantly, also in the case of the lossy interferometry the optimal Kraus operators used in [39] to minimize the asymptotic CE bound satisfy the extra QS’s constraint. This fact indicates that also for  $\varphi$ -extremal channels QS may prove to be as good as CE. However, in the case of spontaneous emission, the QS



Noise model	Dephasing	Depolarization	Loss	Spontaneous emission
$\chi[\Lambda_\varphi]$	$= \sqrt{\frac{1}{1-\eta^2}}$	$\leq \sqrt{\frac{2}{(1-\eta)(1+2\eta)}}$	$= \sqrt{\frac{1}{1-\eta}}$	$\leq \sqrt{\frac{4}{1-\eta}}$
$\chi[\Lambda_\varphi \otimes \mathcal{I}]$	$= \sqrt{\frac{1}{1-\eta^2}}$	$= \sqrt{\frac{1+\eta}{(1-\eta)(1+2\eta)}}$	$= \sqrt{\frac{1}{1-\eta}}$	$= \sqrt{\frac{1+\sqrt{\eta}}{1-\sqrt{\eta}}}$

**Table 2. Quantum phase estimation precision enhancement from the CE method.** For all noise models specified in Appendix A, the asymptotic CE bounds on the maximal quantum precision enhancement factors,  $\chi[\bullet] = \sqrt{\mathcal{F}_{\text{as}}[\bullet]/\mathcal{F}[\bullet]}$ , are presented. For a general quantum map  $\Lambda_\varphi$ , the CE bound only upper-limits  $\chi[\Lambda_\varphi]$  as  $\mathcal{F}_{\text{as}}[\Lambda_\varphi] \leq \mathcal{F}_{\text{as}}^{\text{CE}}$ . Yet, for dephasing and lossy interferometry, as indicated by “=”, the corresponding values of  $\chi[\Lambda_\varphi]$  have been shown to be attainable [73, 74]. For an extended channel,  $\chi[\Lambda_\varphi \otimes \mathcal{I}]$  is determined by the CE bound as  $\mathcal{F}_{\text{as}}[\Lambda_\varphi \otimes \mathcal{I}] = \mathcal{F}_{\text{as}}^{\text{CE}}$ .

method ceases to work, as the  $\beta_{\tilde{K}} = 0$  condition fixes  $\alpha_{\tilde{K}}$  to be disproportional to identity [39].

#### 4.1.3. Channel extension (CE) method

The CE method of [39] not only applies to the widest class of quantum maps containing all  $\varphi$ -non-extremal ones, but also provides more stringent bounds than the CS, RLD and QS equivalents, as respectively proven in [39], Appendix C and above. In this method, see Figure 1b, each single channel is extended by an auxiliary ancilla as introduced in Section 3.3. In [35], it has been proven that one can then effectively bound the  $N$ -channel QFI (15) via the  $N$ -extended-channel QFI, so that

$$\mathcal{F}[\Lambda_\varphi^{\otimes N}] \leq \mathcal{F}[(\Lambda_\varphi \otimes \mathcal{I})^{\otimes N}] \leq 4 \min_h \{N \|\alpha_{\tilde{K}}\| + N(N-1) \|\beta_{\tilde{K}}\|^2\}, \quad (23)$$

where again  $\alpha_{\tilde{K}} = \sum_{i=1}^r \dot{K}_i(\varphi)^\dagger \dot{K}_i(\varphi)$ ,  $\beta_{\tilde{K}} = i \sum_{i=1}^r \dot{K}_i(\varphi)^\dagger \tilde{K}_i(\varphi)$  and  $h$  is the generator of local Kraus representation rotations (9). Crucially, if there exists a Kraus representation for which the second term in (23) vanishes,  $\mathcal{F}[\Lambda_\varphi^{\otimes N}]$  must asymptotically scale linearly in  $N$ . This requirement corresponds to the constraint  $\beta_{\tilde{K}} = 0$  already accounted in the QS method, which for any linearly independent Kraus operators  $\{K_i\}_{i=1}^r$  is equivalent to the existence of  $h$  such that [35]

$$\sum_{i,j=1}^r h_{ij} K_i^\dagger K_j = i \sum_{i=1}^r \dot{K}_i(\varphi)^\dagger \dot{K}_i(\varphi). \quad (24)$$

What is more, for any channel that admits an  $h$  fulfilling (24), one can show basing on the results of [35] that the second inequality in (23) is saturated in the  $N \rightarrow \infty$  limit, so that the *asymptotic extended channel QFI* then reads

$$\mathcal{F}_{\text{as}}[\Lambda_\varphi \otimes \mathcal{I}] = \lim_{N \rightarrow \infty} \frac{\mathcal{F}[(\Lambda_\varphi \otimes \mathcal{I})^{\otimes N}]}{N} = 4 \min_{\substack{h \\ \beta_{\tilde{K}}=0}} \left\| \sum_{i=1}^r \dot{K}_i(\varphi)^\dagger \dot{K}_i(\varphi) \right\|. \quad (25)$$

Importantly, (25) becomes the required asymptotic bound  $\mathcal{F}_{\text{as}}^{\text{bound}}$  of (18), which we refer to as the *asymptotic CE bound*— $\mathcal{F}_{\text{as}}^{\text{CE}}$ . We explicitly wrote the full form of (25) to emphasize its similarity to the extended *single* channel QFI (12). The essential difference in (25) is the constraint (24) yielding  $\mathcal{F}_{\text{as}}[\Lambda_\varphi \otimes \mathcal{I}] \geq \mathcal{F}[\Lambda_\varphi \otimes \mathcal{I}]$  and dictating the maximal quantum precision enhancement for an extended channel:

$$\chi[\Lambda_\varphi \otimes \mathcal{I}] = \lim_{N \rightarrow \infty} \frac{\Delta \tilde{\varphi}_{\text{cl}}^{\text{ext}}}{\Delta \tilde{\varphi}_{\text{Q}}^{\text{ext}}} = \sqrt{\frac{\mathcal{F}_{\text{as}}[\Lambda_\varphi \otimes \mathcal{I}]}{\mathcal{F}[\Lambda_\varphi \otimes \mathcal{I}]}} \geq 1. \quad (26)$$

Similarly to (12), (25) is computable by means of semi-definite programming [39], so that one can efficiently determine both (18) and (26). The CE-based bounds on  $\chi[\Lambda_\varphi]$  and the exact values of  $\chi[\Lambda_\varphi \otimes \mathcal{I}]$  for the relevant noise models are presented in Table 2. Although generally the CE method only upper-limits the maximal quantum precision enhancement (17), it has been proven to quantify  $\chi[\Lambda_\varphi]$  exactly in the case of dephasing [73] and lossy interferometer channels [74]. This has been achieved by showing that input states utilizing spin- and light- squeezing respectively yield a quantum enhancement that asymptotically attains the corresponding CE-based bounds presented in Table 2. On the other hand, as indicated in Table 1, these channels are also examples of ones for which the extension does not improve the precision at the single channel level, so that  $\chi[\Lambda_\varphi] = \chi[\Lambda_\varphi \otimes \mathcal{I}]$  in Table 2. The question—when the lack of precision improvement due to extension at the single channel level translates to the asymptotic regime, i.e.  $\mathcal{F}[\Lambda_\varphi] = \mathcal{F}[\Lambda_\varphi \otimes \mathcal{I}] \stackrel{?}{\iff} \mathcal{F}_{\text{as}}[\Lambda_\varphi] = \mathcal{F}_{\text{as}}[\Lambda_\varphi \otimes \mathcal{I}]$ , we leave open for future research.

#### 4.2. Finite- $N$ channel extension (CE) method

In Section 4.1, we have presented the CE method as the most effective one out of all discussed that provides the tightest upper limits on the maximal possible asymptotic quantum precision enhancement. On the other hand, in the case of experiments such as optical interferometry with moderate numbers of photons [8, 9], the asymptotic CE bounds, despite still being valid, are far too weak to be useful. For very low values of  $N$ , the precision can be quantified numerically, for instance by brute-force type methods computing explicitly the QFI. However, in the intermediate  $N$  regime—being beyond the reach of computational power, yet with  $N$  too low for the asymptotic methods to be effective—more accurate bounds should play an important role.

We propose the finite- $N$  CE method which, despite being based on the properties of a single channel, still provides bounds on precision that are relevant in the intermediate  $N$  regime. We utilize the upper-limit (23) on the  $N$ -extended-channel QFI and construct the *finite- $N$  CE bound*,  $\mathcal{F}_N^{\text{CE}}$ , that reads

$$\frac{\mathcal{F}\left[(\Lambda_\varphi \otimes \mathcal{I})^{\otimes N}\right]}{N} \leq \mathcal{F}_N^{\text{CE}} = 4 \min_h \left\{ \|\alpha_{\tilde{K}}\| + (N-1) \|\beta_{\tilde{K}}\|^2 \right\}. \quad (27)$$

Following the suggestion of [39], in contrast to the asymptotic CE bound  $\mathcal{F}_{\text{as}}^{\text{CE}}$  defined in (25), we do not impose the SQL-bounding condition  $\beta_{\tilde{K}} = 0$  (24), but we seek at each  $N$  for the minimal Kraus representation that is generated by some optimal  $h = h_{\text{opt}}(N)$

being now not only channel but also  $N$ -dependent. Still, as shown in Appendix E,  $\mathcal{F}_N^{\text{CE}}$  can always be efficiently evaluated numerically by recasting the minimization over  $h$  in (27) into a semi-definite programming task. Moreover, as the finite- $N$  CE bound varies smoothly between  $N = 1$  and  $N = \infty$ , at which it is tight, it provides more accurate bounds than its asymptotic version. For  $N = 1$ ,  $\mathcal{F}_N^{\text{CE}}$  coincides with the extended channel QFI (12)— $\mathcal{F}_{N=1}^{\text{CE}} = \mathcal{F}[\Lambda_\varphi \otimes \mathcal{I}]$ , whereas in the  $N \rightarrow \infty$  limit it attains the asymptotic CE bound (25)— $\mathcal{F}_{N \rightarrow \infty}^{\text{CE}} = \mathcal{F}_{\text{as}}^{\text{CE}}$ .

What is more, when considering channels for which the asymptotic CE method fails, as it is not possible to set  $\beta_{\tilde{K}} = 0$  in (23) for any Kraus representation, (27) still applies; it is the finite- $N$  CE method that provides the correct CE-based bound in the  $N \rightarrow \infty$  limit that in principle may then surpass the SQL-like scaling. On the other hand, when dealing with estimation schemes in which one can moderate the effective amount of loss (i.e. the form of  $\Lambda_\varphi$ ) depending on the number of particles, the asymptotic bound  $\mathcal{F}_{\text{as}}^{\text{CE}}$  may not actually be the tightest within the CE method. The  $\beta_{\tilde{K}}$  of (23) and (27) becomes then a function of  $N$  and it may not be asymptotically optimal to set it equal to zero by imposing condition (24). Yet the finite- $N$  CE method, being not constrained with  $\beta_{\tilde{K}} = 0$ , still yields the correct CE-based bound on precision as  $N \rightarrow \infty$ . This fact has been utilized in [40], where, owing to the  $N$ -dependence of  $\beta_{\tilde{K}}$ , the finite- $N$  CE method provided an asymptotic bound indeed tighter than the naively calculated  $\mathcal{F}_{\text{as}}^{\text{CE}}$ . What is more, the  $\mathcal{F}_{N \rightarrow \infty}^{\text{CE}}$  has been numerically shown there to be saturable, what proves the power of the more agile finite- $N$  CE method. For phase estimation with various decoherence models including dephasing, depolarization, loss and spontaneous emission described in detail in Appendix A, we observe that the finite- $N$  CE bound is simply related to its asymptotic form as

$$\mathcal{F}_N^{\text{CE}} = \frac{N \mathcal{F}_{\text{as}}^{\text{CE}}}{N + \mathcal{F}_{\text{as}}^{\text{CE}}}, \quad (28)$$

where one should substitute for  $\mathcal{F}_{\text{as}}^{\text{CE}}$  the corresponding asymptotic CE bounds presented in Table 1 ‡. For dephasing and loss decoherence models, we show explicitly in Figure 3 both the asymptotic and the finite- $N$  bounds accompanied by the plots of actual precision achievable with explicit estimation strategies optimal either in the small or large  $N$  regime.

In the first case, depicted in Figure 3a, we consider a Ramsey spectroscopy setup of [13, 14] in which the probe consists of atoms prepared in a spin-squeezed state [73]. The parameter is then encoded in the phase of a unitary rotation generated by the total angular momentum of the atoms that simultaneously experience uncorrelated dephasing. After measuring probe's total angular momentum perpendicular to the one generating the estimated phase change, the parameter is reconstructed with uncertainty plotted in Figure 3a. For comparison, the maximal precision theoretically achievable with Greenberger-Horne-Zeilinger (GHZ) [75] input states is also shown. The QFI for a

‡ In the case of spontaneous emission noise the formula is valid only for  $N \geq 2$ , what we suspect to be a consequence of the spontaneous emission channel being an extremal map [61].

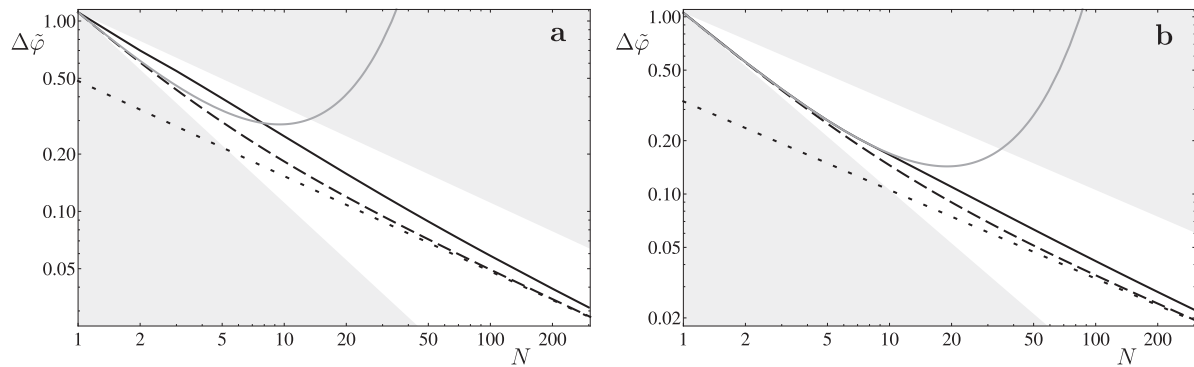


**Figure 3. Phase estimation CE method-based bounds on precision**

(a) *Dephasing*: Finite- $N$  (dashed) and the asymptotic CE bounds (dotted) on estimation uncertainty as compared with the precision achieved by utilizing spin-squeezed states in a Ramsey spectroscopy setup (solid black) and GHZ states with optimal measurement (solid grey) for a probe consisting of  $N$  atoms experiencing uncorrelated dephasing with  $\eta = 0.9$ .

(b) *Loss*: Lossy interferometry with particle survival probability  $\eta = 0.9$ , e.g. Mach-Zehnder interferometer experiencing photonic loss in both of its arms, with effective power transmission  $\eta$ . The smallest uncertainty in a phase estimation scheme is quantified by calculating the QFI for numerically optimized  $N$ -particle input states (solid black) which only at low  $N$  can be approximated by N00N states (solid grey). Again, finite- $N$  (dashed) and asymptotic CE bounds (dotted) on precision are shown for comparison.

GHZ-based strategy is  $\mathcal{F}_N^{\text{GHZ}} = \eta^{2N} N^2$  which for low  $N$  attains the finite- $N$  CE bound. This fact proves that in experiments with only few particles involved, such as [1], it is optimal to use the GHZ states as inputs despite the uncorrelated dephasing present.

In the second lossy interferometry case, shown in Figure 3b, each particle is subject to an independent loss process with survival probability  $\eta$ , as in e.g. Mach-Zehnder interferometer with effective power transmittance  $\eta$  in both arms [29, 30] that represents preparation, transmission and detection loss [31]. Here the solid black line represents the maximal QFI achieved with numerically optimised  $N$ -particle or equivalently  $N$ -photon states ††. As expected, it coincides for low  $N$  with the QFI attained by the so called N00N states [76],  $\mathcal{F}_N^{\text{N00N}} = \eta^N N^2$ , which are the optical equivalents of the GHZ states previously considered. The plot indicates that the finite- $N$  CE bound may be considered in this case to be tight only for moderate and very large  $N$ . Although in the case of lossy optical interferometry, the maximal quantum enhancement of Table 2 can also be achieved via an estimation strategy that employs squeezed-light as the input with mean number of photons constrained to  $N = \bar{N}$  [74, 77], we cannot compare its precision with the one bounded through  $\mathcal{F}_{N=\bar{N}}^{\text{CE}}$ . As  $N \cdot \mathcal{F}_N^{\text{CE}}$  is a convex quantity in  $N$ , one cannot use it naively to constrain precision after replacing  $N$  by the mean number of photons  $\bar{N}$ . This contrasts the case of the (constant) asymptotic CE bound, which yields  $N \cdot \mathcal{F}_{\text{as}}^{\text{CE}}$  being linear in  $N$ , so that it also applies to estimation strategies employing

††As it is optimal to consider indistinguishable, bosonic particles [30].

states of indefinite photon number, as pointed in [39, 77].

## 5. Frequency estimation in atomic models

We apply the methods discussed above to the case of frequency estimation problems in atomic spectroscopy. The general Ramsey spectroscopy setup considered in [13, 14, 22–26, 40] corresponds to  $N$  identical two-level atoms—spin-1/2 systems—with their states separated, where typically the detuning  $\omega$  of an external oscillator frequency from the atoms transition frequency is to be estimated. We assume that the full experiment takes an overall time  $T$ , during which the estimation procedure is repeated  $k = T/t$  times, where  $t$  is the evolution duration of each experimental shot. The quantum Cramér-Rao bound (2) on precision of the estimate  $\tilde{\omega}$  can be then conveniently rewritten as

$$\Delta\tilde{\omega} \geq \frac{1}{\sqrt{T f_t[\rho_\omega^N(t)]}}, \quad (29)$$

where  $f_t[\rho(t)] = F_Q[\rho(t)]/t$  is now the effective QFI per shot duration and  $\rho_\omega^N(t)$  denotes the final state of the whole probe containing  $N$  particles being measured in each shot. The total time  $T$  plays then the role of  $k$  in (2) and, after fixing  $t$ , the bound (29) can always be saturated as  $T \rightarrow \infty$ . The evolution of the probe can be modelled by the master equation of the Lindblad [54] form

$$\frac{\partial \rho_\omega^N(t)}{\partial t} = \sum_{n=1}^N i \frac{\omega}{2} [\sigma_3^{(n)}, \rho_\omega^N(t)] + \mathcal{L}^{(n)}[\rho_\omega^N(t)], \quad (30)$$

where  $\sigma_3^{(n)}$  is the Pauli operator generating a unitary rotation of the  $n$ 'th atom around the  $z$  axis in its Bloch ball representation. The uncorrelated noise is represented by the Liouvillian part  $\mathcal{L}^{(n)}$  acting independently on each particle, here the  $n$ 'th, so that effectively  $\rho_\omega^N(t) = \Lambda_{\omega;t}^{\otimes N}[[\psi_{\text{in}}^N]]$  with channel  $\Lambda_{\omega;t}$  representing the overall single particle evolution over time  $t$ . To model the decoherence we consider the dephasing, depolarization, loss and spontaneous emission maps, which corresponding Liouvillians can be found in Appendix A. As the estimated parameter corresponds now to  $\omega = \varphi/t$ , where  $\varphi$  is the phase of the unitary rotation, the QFI via a parameter change just rescales, so that  $f_t[\rho_\omega] = F_Q[\rho_\omega]/t = F_Q[\rho_\varphi] t$ . Moreover, due to the commutativity of the unitary and the considered decoherence maps, we can without loss of generality utilize the results presented for them in the previous sections. Defining the channel QFI for frequency estimation tasks similarly to (7) as

$$\mathfrak{f}[\Lambda_\omega] = \max_{0 \leq t \leq T} \max_{\psi_{\text{in}}} f_t[\Lambda_{\omega;t}[[\psi_{\text{in}}]]] \quad (31)$$

we can compute all the appropriate expressions for QFIs and the asymptotic bounds of Table 1 as well as the finite- $N$  bounds of (28) by substituting for the effective time dependence of the decoherence strength  $\eta(t)$ , which is determined by the master equation (30) (see Appendix A). Then, any quantity  $\mathcal{F}$  listed in Table 1 transforms to its  $t$ -optimized equivalent as  $\mathfrak{f} = \max_{0 \leq t \leq T} \mathcal{F} t$ . In Table 3 we present the channel QFIs relevant for

Noise model	$f[\Lambda_\omega]$	$f[\Lambda_\omega \otimes \mathcal{I}]$	$f_N^{\text{CE}} (N \geq 2)$	$f_{\text{as}}^{\text{CE}}$	$\chi[\Lambda_\omega]$	$\chi[\Lambda_\omega \otimes \mathcal{I}]$
<i>Dephasing</i>	$\frac{1}{2e\gamma}$	$\frac{1}{2e\gamma}$	$\frac{N}{2\gamma} \frac{w_1[N]}{1+(e^{w_1[N]}-1)N}$	$\frac{1}{2\gamma}$	$=\sqrt{e}$	$=\sqrt{e}$
<i>Depolarization</i>	$\frac{3}{4e\gamma}$	$\approx 1.27 \frac{3}{4e\gamma}$	$\frac{3N}{4\gamma} \frac{\alpha w_\beta[N]}{2+(e^{\frac{\alpha}{4}w_\beta[N]}-1)(e^{\frac{\alpha}{4}w_\beta[N]}+2)N}$	$\frac{1}{\gamma}$	$\leq \sqrt{\frac{4e}{3}}$	$\approx 0.89 \sqrt{\frac{4e}{3}}$
<i>Loss</i>	$\frac{1}{e\gamma}$	$\frac{1}{e\gamma}$	$\frac{N}{\gamma} \frac{w_1[N]}{1+(e^{w_1[N]}-1)N}$	$\frac{1}{\gamma}$	$=\sqrt{e}$	$=\sqrt{e}$
<i>Spontaneous emission</i>	$\frac{1}{e\gamma}$	$\frac{4\tilde{w}}{\gamma(1+e^{\tilde{w}/2})^2}$	$\frac{N}{\gamma} \frac{4w_4[N]}{4+(e^{w_4[N]}-1)N}$	$\frac{4}{\gamma}$	$\leq \sqrt{2e}$	$= \frac{1+e^{\tilde{w}/2}}{\sqrt{\tilde{w}}}$

**Table 3. QFIs, CE bounds and quantum enhancements in frequency estimation.** In frequency estimation tasks, the precision is maximized by adjusting the single experimental shot duration  $t$ . The  $t$ -optimised (extended) channel QFIs as well as their finite- $N$  and asymptotic CE bounds are presented, where  $w_x[N] = 1 + W\left[\frac{x-N}{eN}\right]$ ,  $\tilde{w} = 1 + 2W\left[\frac{1}{2\sqrt{e}}\right]$  and  $W[x]$  is the Lambert  $W$  function. As in the case of depolarizing channel not all solutions possess an analytical form, only their numerical approximations are shown with  $\alpha \approx 2.20$  and  $\beta \approx 1.32$ . Right of the double-line the maximal quantum precision enhancements are listed for the maps considered. In the case of dephasing noise the ultimate  $\sqrt{e}$  factor has already been reported in [24, 38]. For unextended depolarization and spontaneous emission maps, the derived enhancement factors may possibly be not achievable.

frequency estimation, their asymptotic and finite- $N$  CE bounds, as well as the maximal quantum precision enhancements for each model considered. In the case of dephasing, we recover the results of [24, 38, 40], whereas for depolarizing, loss and spontaneous emission maps we obtain the QFIs and their bounds, which to our knowledge have not been reported in the literature before. However, similarly to the case of quantum phase estimation summarized in Table 2, the obtained quantum enhancement factors for depolarization and spontaneous emission channels serve only as bounds, as they are not guaranteed to be saturable.

## 6. Estimation of decoherence strength

Lastly, we would like to emphasize that the CS, QS and CE methods described in Section 4 also apply to estimation tasks in which the estimated parameter is not encoded in the unitary, noiseless part of the system evolution. Examples of such schemes are the experimentally motivated ones, in which one tries to quantify the effective strength of noise or loss present in the apparatus. That is why we consider again the channels described in Appendix A, but this time with the parameter to be estimated being the decoherence strength  $\eta$ . This kind of problems has been widely considered not only in the estimation theory [44, 78–80], but also when examining issues of channel discrimination [45, 46] with particular application in quantum reading [50–52]. As compared to unitary rotations, the nature of the estimated parameter is dramatically



Channel considered	$\mathcal{F}[\Lambda_\eta]$	$\mathcal{F}[\Lambda_\eta \otimes \mathcal{I}]$	$\mathcal{F}_{\text{as}}^{\text{CS}} = \mathcal{F}_{\text{as}}^{\text{QS}} = \mathcal{F}_{\text{as}}^{\text{CE}}$
<i>Dephasing</i>	$\frac{1}{1-\eta^2}$	$\frac{1}{1-\eta^2}$	$\frac{1}{1-\eta^2}$ [82]
<i>Depolarization</i>	$\frac{1}{1-\eta^2}$ [70]	$\frac{3}{(1-\eta)(1+3\eta)}$ [70]	$\frac{3}{(1-\eta)(1+3\eta)}$ [35, 82]
<i>Loss</i>	$\frac{1}{\eta(1-\eta)}$	$\frac{1}{\eta(1-\eta)}$	$\frac{1}{\eta(1-\eta)}$
<i>Spontaneous emission</i>	$\frac{1}{\eta(1-\eta)}$ [83]	$\frac{1}{\eta(1-\eta)}$ [83]	$\frac{1}{\eta(1-\eta)}$

**Table 4. Decoherence strength estimation quantified via channel QFIs and their asymptotic bounds.** Definitions of channels listed in the first column can be found in Appendix A. In contrast to phase estimation examples given in Table 1, the variable to be estimated here is the decoherence parameter  $\eta$ , ( $0 \leq \eta < 1$ ). Due to the different nature of the estimated parameter, the geometrical CS method provides bounds that not just most tightly limit the asymptotic extended channel QFIs, but actually coincide with its value. The results prove that only in the case of depolarization channel the precision can be enhanced with the use of quantum estimation strategies, as for all other cases  $\mathcal{F}[\Lambda_\eta] = \mathcal{F}[\Lambda_\eta \otimes \mathcal{I}] = \mathcal{F}_{\text{as}}$ .

different. In unitary parameter case, the use of entangled input state of  $N$  particles results in an effective  $N$ -times higher “angular speed” of rotation leading to the HL in the absence of noise. In decoherence strength estimation tasks, a change in the parameter value can be geometrically interpreted in the space of all valid quantum channels as a “movement” in the direction away from the boundary of the space of the relevant CPTP maps, for which “speed” cannot be naively amplified  $N$ -times when employing  $N$  parallel channels. Hence, as in the case of lossy unitary rotation estimation, the optimal entangled inputs must lead not to scaling but constant factor quantum enhancements, which again can be quantified by the methods of Section 4. This also explains that for all the four noise models considered, the purely geometrical notion of classical simulability is enough to bound most tightly the maximal asymptotic precision of estimation. However, as for them also  $\mathcal{F}_{\text{as}}^{\text{CS}} = \mathcal{F}_{\text{as}}^{\text{QS}} = \mathcal{F}_{\text{as}}^{\text{CE}} = \mathcal{F}[\Lambda_\eta \otimes \mathcal{I}]$ , the CS-based asymptotic quantum enhancement corresponds to the classical estimation strategy that employs independent but extended channels. The fact that factorizable inputs—uncorrelated in between the extended  $N$  channels but possibly requiring entanglement between each single particle and its ancilla—are optimal for noise estimation with extended channels, has already been noticed for the low-noise [81] and generalized Pauli [82] channels, of which the latter contain the dephasing and depolarization maps studied here.

In the case of dephasing channel, we further realize that the extension at the single channel level is also unnecessary, as  $\mathcal{F}[\Lambda_\eta] = \mathcal{F}[\Lambda_\eta \otimes \mathcal{I}] = 1/(1-\eta^2)$ , and the geometrically dictated bound of CS is attainable classically just by employing unentangled qubits in any pure state lying on the Bloch sphere equatorial plane.

Similarly, the spontaneous emission and loss maps also turn out to be fully classical. In the first case, the asymptotic CS bound coincides with the extended and unextended channel QFIs derived in [83], whereas for the loss channel we obtain  $\mathcal{F}_{\text{as}}^{\text{CS}} = \mathcal{F}[\Lambda_\eta] = \mathcal{F}[\Lambda_\eta \otimes \mathcal{I}] = 1/(\eta(1-\eta))$ , which at the single channel level is achieved by a photon in any mixed state with the ancilla being redundant. On the one hand, this emphasizes that entanglement between the photons entering the interferometer is unnecessary and agrees with the results of [78, 79] confirming that the total photon number fluctuations are really the ones that limit the precision. These can be reduced by employing Gaussian states [78] or in principle fully eliminated by the use of Fock states [79] that attain the CS-bound.

The case of depolarization map is different, as it is known that for qubits [70, 84] the precision of estimation may be improved by extending the channel, i.e.  $\mathcal{F}[\Lambda_\eta] < \mathcal{F}[\Lambda_\eta \otimes \mathcal{I}]$ . This leaves the space for possible enhancement thanks to the use of entangled probes *between unextended* channels and indeed this fact has been observed already when considering two depolarization channels used in parallel [70]. The results are summarized in Table 4.

## 7. Further discussion

We would also like to point that the SQL-like bounds, universally valid in practical metrological scenarios, allow one to avoid some of the controversies characteristic for idealized decoherence-free scenarios. When decoherence is *not* present and the probe states with indefinite number of particles are considered, such as e.g. squeezed states of light, the exact form of HL needs to be reconsidered [85–87] since the direct replacement of  $N$  with mean number of particles  $\bar{N}$  may make the HL invalid. Moreover, the final claims on the achievable precision scaling may strongly depend on the form of a priori parameter knowledge assumed, and lead to some apparent contradictions [88, 89]. These difficulties do not arise in the realistic metrological schemes, as the asymptotic SQL-like bounds are valid also when  $N$  is replaced by  $\bar{N}$  for indefinite particle number state [39, 77]. The bounds derived in the *local approach* (small parameter fluctuation) based on the calculation of the QFI are saturable in a single-shot scenario unlike the decoherence-free case when only after some number of independently repeated experiments one may expect to approach the theoretical limits [90, 91]. This is due to the fact that by employing input states of grouped particles, which possess no correlations in between the groupings, and by letting the groups to be of finite but sufficiently large size, one can attain the ultimate asymptotic SQL bound up to any precision. Since saturability of the QFI bounds for independently prepared probes is well established [62–64, 92], the operational meaning of the QFI is also clear in the single shot scenario. The above argument also suggests the asymptotically optimal form of the input states, which should include ones that do not possess long-range correlations in between the particles. This observation has already been made in [93] and indicates that in methods designed to search for the optimal inputs in scenarios with uncorrelated noise one may



restrict himself to states with short-range correlations such as for example the matrix product states of low bond dimensions [94].

We also conjecture from the point of view of the asymptotic SQL-like bounds that the specific form of the *a priori* knowledge should not play an important role. In particular, we expect that various methods such as *Bayesian* [95–98] or *information theoretic* [99, 100] should recover the bounds compatible with the ones obtained via the *local approach* considered in this paper. This statement is known to hold in the case of optical interferometry with losses [31, 32]; it is an intriguing question whether analogous claims can be made in more general scenarios.

## 8. Summary and outlook

We have constructed explicit methods capable of determining fundamental bounds on quantum enhancement in metrological setups in presence of uncorrelated noise. The methods are based on the study of the structure of a single-particle quantum channel that represents the decoherence process. The methods do not require any kind of educated guess, nor an involved numerical optimization—given a set of Kraus operators representing the channel, bounds on precision can be derived immediately without the need to search e.g. for the optimal input states. We have discussed the efficiency of CS, QS, RLD and CE methods in providing asymptotic bounds on precision for phase estimation under a number of different decoherence models. We have also generalized the CE method in order to provide tighter bounds in the regime of finite number of particles and we have showed that this generalization can be again cast in the form of a semi-definite program. The methods have also been applied to a related problem of frequency estimation. Moreover, it has been shown that when thinking of estimation of the decoherence parameter itself already the simplest approach based on the CS method typically provides the tightest bounds. While the methods are efficient as they avoid the search for the optimal many particle input states, formulation of an explicit optimal estimation strategy may in general require performing such a search. Hopefully, the optimal states are expected to have a relatively simple structure and can be searched within a restricted class of states such as e.g. squeezed or matrix product states [73, 77, 93, 94]. Once the precision calculated for a given input state hits the fundamental bound one is guaranteed that the optimal strategy has been identified. The natural future work on our methods is to generalize them and study their applicability in the multi-parameter estimation schemes where it is *a priori* not clear which of the different approaches will be the most fruitful and whether some nontrivial new bounds may be derived.

## Acknowledgments

We would like to thank Mădălin Guță and Lorenzo Maccone for valuable feedback as well as Konrad Banaszek for constant support. J.K. also acknowledges Michal Sedlák

and Jonatan Bohr Brask for helpful comments and thanks Marcin Jarzyna for many fruitful discussions as well as the data utilized in Figure 3. This research was supported by Polish NCBiR under the ERA-NET CHIST-ERA project QUASAR, Foundation for Polish Science TEAM project co-financed by the EU European Regional Development Fund and FP7 IP project Q-ESSENCE.

## Appendix A. Channels considered

We adopt the standard notation in which  $\mathbb{I}_d$  represents a  $d \times d$  identity matrix and  $\{\sigma_i\}_{i=1}^3$  are the Pauli operators. In Section 4.2 parameter  $\varphi$  to be estimated is the rotation angle around the  $z$  axis of the Bloch ball generated by the unitary operator  $U_\varphi = \exp[i\sigma_3\varphi/2]$ . We consider maps  $\mathcal{D}_\eta$  with decoherence parameter  $\eta$  that commute with such rotation, whence  $\Lambda_\varphi[\varrho] = \mathcal{D}_\eta[U_\varphi\varrho U_\varphi^\dagger] = U_\varphi\mathcal{D}_\eta[\varrho]U_\varphi^\dagger$ , and are defined accordingly by the Kraus operators presented below. For each case, we also specify the purification determining the extended channel QFI (12) ( $\mathcal{F}[\Lambda_\varphi \otimes \mathcal{I}]$  in Table 1) in the form of the optimal generator of Kraus representation rotation  $h$ , as introduced in (10). Dealing with frequency estimation tasks discussed in Section 5 we construct the effective one-particle Kraus operators by substituting  $\varphi \rightarrow \omega t$  and  $\eta \rightarrow \eta(t)$  in the nominal ones, where  $\omega$  is the estimated frequency detuning. For all models, we explicitly write the Liouvillian  $\mathcal{L}^{(n)}$  determining the noise affecting each particle, see (30), and the effective form of  $\eta(t)$ . When discussing decoherence strength estimation in Section 6, we consider solely each of the following noise maps with  $\eta$  being now the parameter to be estimated:  $\Lambda_{\varphi=\eta} = \mathcal{D}_\eta$ .

### Appendix A.1. Dephasing

- *Decoherence parameter*,  $\eta$ , represents the final equatorial radius of the Bloch ball shrank uniformly in the  $xy$  plane by the channel.
- *Kraus operators*:

$$K_1 = \sqrt{\frac{1+\eta}{2}} \mathbb{I}_2, \quad K_2 = \sqrt{\frac{1-\eta}{2}} \sigma_3. \quad (\text{A.1})$$

- *Optimal purification* determining the extended channel QFI (12):

$$h = \frac{\sqrt{1-\eta^2}}{2} \sigma_1. \quad (\text{A.2})$$

- *One-particle Liouvillian* for frequency estimation tasks:

$$\mathcal{L}^{(n)}[\varrho] = \frac{\gamma}{2} \left( \sigma_3^{(n)} \varrho \sigma_3^{(n)} - \varrho \right) \quad \therefore \quad \eta(t) = e^{-\gamma t}. \quad (\text{A.3})$$

### Appendix A.2. Depolarization

- *Decoherence parameter*,  $\eta$ , represents the final radius of the Bloch ball shrunk isotropically by the channel.

- *Kraus operators:*

$$K_1 = \sqrt{\frac{1+3\eta}{4}} \mathbb{I}_2, \quad \left\{ K_i = \sqrt{\frac{1-\eta}{4}} \sigma_{i-1} \right\}_{i=2\dots 4}. \quad (\text{A.4})$$

- *Optimal purification* determining the extended channel QFI (12):

$$h = \frac{1}{2} \begin{pmatrix} 0 & 0 & 0 & \xi \\ 0 & \begin{bmatrix} \sigma_2 \end{bmatrix} & 0 \\ 0 & \begin{bmatrix} \sigma_2 \end{bmatrix} & 0 \\ \xi & 0 & 0 & 0 \end{pmatrix} \quad \text{with} \quad \xi = \frac{\sqrt{(1+3\eta)(1-\eta)}}{1+\eta}. \quad (\text{A.5})$$

- *One-particle Liouvilian* for frequency estimation tasks:

$$\mathcal{L}^{(n)}[\varrho] = \frac{\gamma}{2} \left( \frac{1}{3} \sum_{i=1}^3 \sigma_i^{(n)} \varrho \sigma_i^{(n)} - \varrho \right) \quad \therefore \quad \eta(t) = e^{-\frac{2\gamma}{3}t}. \quad (\text{A.6})$$

### Appendix A.3. Loss

- *Decoherence parameter*,  $\eta$ , represents survival probability of each of the particles that are subject to independent loss processes. The channel on a single particle is formally a map from a two- to a three-dimensional system with the output's third dimension corresponding to the vacuum mode responsible for the particle loss. Although in this case one should strictly write  $\Lambda_\varphi = \mathcal{D}_\eta[U_\varphi \varrho U_\varphi^\dagger] = \tilde{U}_\varphi \mathcal{D}_\eta[\varrho] \tilde{U}_\varphi^\dagger$  with  $\tilde{U}_\varphi$  acting on a different Hilbert space, the effects of  $U_\varphi$  and  $\tilde{U}_\varphi$  are physically indistinguishable, as the particle losses commute with the acquired phase (for instance see [30]). In the case of optical interferometry,  $\eta$  represents the effective power transmittance assumed to be equal in both arms and accounts for preparation and transmission loss as well as detector inefficiencies in a Mach-Zehnder setup [31].
- *Kraus operators:*

$$K_1 = \begin{pmatrix} 0 & 0 \\ 0 & 0 \\ 0 & \sqrt{1-\eta} \end{pmatrix}, \quad K_2 = \begin{pmatrix} 0 & 0 \\ 0 & 0 \\ \sqrt{1-\eta} & 0 \end{pmatrix}, \quad K_3 = \begin{pmatrix} \sqrt{\eta} & 0 \\ 0 & \sqrt{\eta} \\ 0 & 0 \end{pmatrix}. \quad (\text{A.7})$$

- *Optimal purification* determining the extended channel QFI (12):

$$h = -\frac{1}{2} \begin{pmatrix} \begin{bmatrix} \sigma_3 \end{bmatrix} & 0 \\ \begin{bmatrix} \sigma_3 \end{bmatrix} & 0 \\ 0 & 0 & 0 \end{pmatrix}. \quad (\text{A.8})$$

- *One-particle Liouvilian* for the frequency estimation tasks:

$$\mathcal{L}^{(n)}[\varrho] = \gamma \sum_{m=0}^1 \left( \sigma_{m,+}^{(n)} \varrho \sigma_{m,-}^{(n)} - \frac{1}{2} \left\{ \sigma_{m,-}^{(n)} \sigma_{m,+}^{(n)}, \varrho \right\} \right) \quad \therefore \quad \eta(t) = e^{-\gamma t}, \quad (\text{A.9})$$

where  $\sigma_{m,+}^{(n)} = |\text{vac}\rangle\langle m|$  are the generators of transition to the vacuum mode from qubit basis states  $|0\rangle$  and  $|1\rangle$ , such that  $\sigma_{m,-}^{(n)} = \sigma_{m,+}^{(n)\dagger}$ .

The methods discussed in the paper may also be easily applied to more general loss models such as: unequal loss in the two arms of an interferometer [29] or the models with distinguished preparation, transmission and detection loss [101]. For the conciseness of the paper, however, we restrict ourselves to the simplest loss model described above.

#### Appendix A.4. Spontaneous emission (amplitude damping)

- *Decoherence parameter*,  $\eta$ , represents the radius of the disk obtained by projecting the deformed Bloch ball outputted by the channel onto the  $xy$  plane.
- *Kraus operators*:

$$K_1 = \begin{pmatrix} 1 & 0 \\ 0 & \sqrt{\eta} \end{pmatrix}, \quad K_2 = \begin{pmatrix} 0 & \sqrt{1-\eta} \\ 0 & 0 \end{pmatrix}. \quad (\text{A.10})$$

- *Optimal purification* determining the extended channel QFI (12):

$$h = \frac{1}{2} \begin{pmatrix} \xi & 0 \\ 0 & -1 \end{pmatrix} \quad \text{with} \quad \xi = \frac{1 - \sqrt{\eta}}{1 + \sqrt{\eta}}. \quad (\text{A.11})$$

- *One-particle Liouvillian* for the frequency estimation tasks ( $\sigma_{\pm} = \frac{1}{2}(\sigma_1 \pm i\sigma_2)$ ):

$$\mathcal{L}^{(n)}[\rho] = \gamma \left( \sigma_+^{(n)} \rho \sigma_-^{(n)} - \frac{1}{2} \left\{ \sigma_-^{(n)} \sigma_+^{(n)}, \rho \right\} \right) \quad \therefore \quad \eta(t) = e^{-\gamma t}. \quad (\text{A.12})$$

## Appendix B. Equivalence of RLD-based bound applicability and local classical simulability of a channel

Given a channel—a CPTP map  $\Lambda_\varphi: \mathcal{H}_{\text{in}} \rightarrow \mathcal{H}_{\text{out}}$ —we define its C-J matrix representation [61] as  $\Omega_{\Lambda_\varphi} = \Lambda_\varphi \otimes \mathcal{I} [|\mathbb{I}\rangle\langle\mathbb{I}|] = \sum_i |K_i(\varphi)\rangle\langle K_i(\varphi)|$ , where  $\{K_i(\varphi)\}_{i=1}^r$  are  $r$  linearly independent Kraus operators of  $\Lambda_\varphi$ ; we adopt a concise notation for bipartite states, in which  $|\phi\rangle = \sum_{i,j=1}^{\dim \mathcal{H}_{\text{in}}} \langle i|\phi|j\rangle |i\rangle|j\rangle = \phi \otimes \mathbb{I} |\mathbb{I}\rangle = \mathbb{I} \otimes \phi^T |\mathbb{I}\rangle$  with  $|\mathbb{I}\rangle = \sum_{i=1}^{\dim \mathcal{H}_{\text{in}}} |i\rangle|i\rangle$ . For simplicity, from now onwards we drop the explicit  $\varphi$  dependence of operators, assuming that the estimation is performed for small variations  $\delta\varphi$  around a given, fixed  $\varphi$ . In Sup. Mat. of [39] (Equation (S9)) it has been proven that the condition for any channel to be  $\varphi$ -non-extremal at  $\varphi$  is equivalent to the statement that there exists a non-zero Hermitian matrix  $\mu_{ij}$  such that

$$\dot{\Omega}_{\Lambda_\varphi} = \sum_{ij} \mu_{ij} |K_i\rangle\langle K_j|. \quad (\text{B.1})$$

On the other hand, the RLD-based bound exists there if and only if [37]

$$P_{\Omega_\perp} \dot{\Omega}_{\Lambda_\varphi}^2 P_{\Omega_\perp} = 0 \quad (\text{B.2})$$

where  $P_{\Omega_\perp}$  is the projection onto the null-space  $\Omega_\perp$ , i.e. the subspace orthogonal to  $\Omega_{\Lambda_\varphi}$ , so that  $\forall_i: P_{\Omega_\perp} |K_i\rangle = 0$ . The (B.1) implies (B.2), as by substitution

$$P_{\Omega_\perp} \left( \sum_{ij} \mu_{ij} |K_i\rangle\langle K_j| \right)^2 P_{\Omega_\perp} = \sum_{ij} \left( \sum_p \mu_{ip} \langle K_p|K_p\rangle \mu_{pj} \right) P_{\Omega_\perp} |K_i\rangle\langle K_j| P_{\Omega_\perp} = 0, \quad (\text{B.3})$$

thus any  $\varphi$ -non-extremal channel must admit an RLD-based bound on its extended QFI. In order to prove the other direction, we split the derivatives of each C-J eigenvector into components supported by  $\Omega_{\Lambda_\varphi}$  and in the null-space  $\Omega_\perp$ :  $|\dot{K}_i\rangle = \sum_j \nu_{ij} |K_j\rangle + |K_i^\perp\rangle$ . Hence, after substituting for  $\dot{\Omega}_{\Lambda_\varphi}$  the (B.2) then simplifies to

$$\left( \sum_i |K_i^\perp\rangle \langle K_i| \right) \left( \sum_j |K_j\rangle \langle K_j^\perp| \right) = 0, \quad (\text{B.4})$$

and since  $A^\dagger A = 0$  implies  $A^\dagger = A = 0$  and  $\{|K_i\rangle\}_i$  are orthogonal, we conclude that all  $|K_i^\perp\rangle = 0$ . Thus, (B.2) implies that  $|\dot{K}_i\rangle = \sum_j \nu_{ij} |K_j\rangle$ , which due to the local ambiguity of Kraus representations (9) is equivalent to  $|\dot{K}_i\rangle = \sum_j (\nu_{ij} - i h_{ij}) |\tilde{K}_j\rangle$  for any Hermitian  $h$ . Therefore, without loss of generality, we may set  $h = -\frac{i}{2} \nu^{\text{AH}}$  after splitting  $\nu$  into its Hermitian and anti-Hermitian parts  $\nu = \nu^{\text{H}} + \nu^{\text{AH}}$ , so that  $|\dot{K}_i\rangle = \sum_j \nu_{ij}^{\text{H}} |\tilde{K}_j\rangle$  with  $\nu^{\text{H}} \neq 0$  for any non-trivial channel. Finally, we can write

$$\dot{\Omega}_\varphi = \sum_i |\dot{K}_i\rangle \langle \tilde{K}_i| + |\tilde{K}_i\rangle \langle \dot{K}_i| = 2 \sum_{ij} \nu_{ji}^{\text{H}} |\tilde{K}_i\rangle \langle \tilde{K}_j| \quad (\text{B.5})$$

and satisfy the condition (B.1). ■

### Appendix C. RLD-based bound as a special case of asymptotic CE bound

For a channel that admits an RLD-based bound, in order to obtain the CS condition (B.5) in Appendix B, we chose  $h = -\frac{i}{2} \nu^{\text{AH}}$  that actually satisfies the  $\beta_{\tilde{K}} = 0$  constraint (24) of the CE method. This can be verified by taking the  $\text{Tr}_{\mathcal{H}_{\text{out}}}\{\dots\}$  of the both sides of the identity

$$\sum_{ij} h_{ij} |K_j\rangle \langle K_i| = \sum_{ij} \frac{i}{2} (\nu_{ij} - \nu_{ij}^\dagger) |K_j\rangle \langle K_i| = \frac{i}{2} \sum_i |\dot{K}_i\rangle \langle K_i| - |K_i\rangle \langle \dot{K}_i|, \quad (\text{C.1})$$

which results in (24). This is consistent, as the CE method must apply to any  $\varphi$ -non-extremal channel [39] admitting an RLD-based bound. Furthermore, the asymptotic CE bound (25) is at least as tight as the RLD-based bound (13) on the extended channel QFI (12). We prove this by substituting (B.5) into the definition of  $\mathcal{F}^{\text{RLD}}[\Lambda_\varphi \otimes \mathcal{I}]$  in (13), so that

$$\mathcal{F}^{\text{RLD}}[\Lambda_\varphi \otimes \mathcal{I}] = 4 \left\| \text{Tr}_{\mathcal{H}_{\text{out}}} \left\{ \sum_{ij} \nu_{ji}^{\text{H}} |\tilde{K}_i\rangle \sum_{pq} \nu_{pq}^{\text{H}} \langle \tilde{K}_q| \right\} \right\| = 4 \left\| \sum_i \dot{K}_i^\dagger \dot{K}_i \right\|, \quad (\text{C.2})$$

where we have used the fact that  $\langle \tilde{K}_j | \Omega_\varphi^{-1} | \tilde{K}_p \rangle = \delta_{jp}$ . Hence,  $\mathcal{F}^{\text{RLD}}[\Lambda_\varphi \otimes \mathcal{I}]$  is an example of an asymptotic CE-based bound with a possibly sub-optimal Kraus representation chosen such that  $\forall_i : |\dot{K}_i\rangle = \sum_j \nu_{ij}^{\text{H}} |\tilde{K}_j\rangle$  and  $\beta_{\tilde{K}} = 0$ . ■

## Appendix D. Optimal local QS of a channel

A channel  $\Lambda_\varphi$  of rank  $r$ , in order to be locally *quantum simulable* within small deviations  $\delta\varphi$  from a given  $\varphi$ , must fulfil the condition (see Section 4.1.2)

$$\Lambda_\varphi[\varrho] = \text{Tr}_{\mathbb{E}_\Phi \mathbb{E}_\sigma} \{ U (\varrho \otimes |\psi_\varphi\rangle\langle\psi_\varphi|) U^\dagger \} + O(\delta\varphi^2) = \sum_{i=1}^{r' \geq r} \bar{K}_i(\varphi) \varrho \bar{K}_i(\varphi)^\dagger + O(\delta\varphi^2), \quad (\text{D.1})$$

where  $\bar{K}_i(\varphi) = \langle i|U|\psi_\varphi\rangle$  and  $\{|i\rangle\}_{i=1}^{r'}$  form any basis in the  $r'$  dimensional  $\mathcal{H}_{\mathbb{E}_\Phi} \times \mathcal{H}_{\mathbb{E}_\sigma}$  space containing  $\psi_\varphi$ . Hence,  $\Lambda_\varphi$  must admit a Kraus representation  $\{\tilde{K}_i\}_{i=1}^{r'}$  (with possibly linearly dependent Kraus operators, as for generality we assume  $r' \geq r$ ) that coincides with the one of (D.1) up to  $O(\delta\varphi^2)$ , i.e. satisfies  $\tilde{K}_i = \bar{K}_i$  and  $\dot{\tilde{K}}_i = \dot{\bar{K}}_i$  for all  $i$ . We construct a valid decomposition of  $|\dot{\psi}_\varphi\rangle$  into its (normalized) components parallel and perpendicular to  $\psi_\varphi$ :  $|\dot{\psi}_\varphi\rangle = ia|\psi_\varphi\rangle - ib|\psi_\varphi^\perp\rangle$ , where we can choose  $a, b \in \mathbb{R}$  because of  $\partial_\varphi \langle \psi_\varphi | \dot{\psi}_\varphi \rangle = 0$  and the irrelevance of the global phase. Then, the asymptotic bound  $\mathcal{F}_{\text{as}}^{\text{bound}}$  of (18) determined by the local QS (D.1) at  $\varphi$  simply reads  $F_Q[|\psi_\varphi\rangle] = 4b^2$  and the required Kraus operators  $\{\tilde{K}_i\}_{i=1}^{r'}$  of  $\Lambda_\varphi$  must fulfil conditions  $\tilde{K}_i = \langle i|U|\psi_\varphi\rangle$  and  $\dot{\tilde{K}}_i = \langle i|U|\dot{\psi}_\varphi\rangle = ia\tilde{K}_i - ib\langle i|U|\psi_\varphi^\perp\rangle$ . Hence, for the local QS of channel  $\Lambda_\varphi$  to be valid  $b$  must be finite and we must be always able to construct

$$U = \begin{bmatrix} \tilde{K}_1 & \frac{a}{b}\tilde{K}_1 + \frac{i}{b}\dot{\tilde{K}}_1 & \bullet & \dots & \bullet \\ \tilde{K}_2 & \frac{a}{b}\tilde{K}_2 + \frac{i}{b}\dot{\tilde{K}}_2 & \bullet & \dots & \bullet \\ \tilde{K}_3 & \frac{a}{b}\tilde{K}_3 + \frac{i}{b}\dot{\tilde{K}}_3 & \vdots & \ddots & \vdots \\ \vdots & \vdots & \bullet & \dots & \bullet \end{bmatrix} \quad (\text{D.2})$$

with first two columns fixed to give for all  $i$  the correct  $\langle i|U|\psi_\varphi\rangle$  and  $\langle i|U|\psi_\varphi^\perp\rangle$  respectively. Due to locality, all entries marked with  $\bullet$  in (D.2) can be chosen freely to satisfy the unitarity condition  $U^\dagger U = U U^\dagger = \mathbb{I}$ . Yet, this constraint still requires the Kraus operators to simultaneously fulfil  $i \sum_{i=1}^{r'} \dot{\tilde{K}}_i^\dagger \tilde{K}_i = a \mathbb{I}$  and  $\sum_{i=1}^{r'} \dot{\tilde{K}}_i^\dagger \dot{\tilde{K}}_i = (b^2 + a^2) \mathbb{I}$ . Without loss of generality, we may shift their phase at  $\varphi$ , so that  $\tilde{K}_i \rightarrow e^{-ia\varphi} \tilde{K}_i$  and the conditions become independent of  $a$ , i.e.  $i \sum_{i=1}^{r'} \dot{\tilde{K}}_i^\dagger \tilde{K}_i = 0$  and  $\sum_{i=1}^{r'} \dot{\tilde{K}}_i^\dagger \dot{\tilde{K}}_i = b^2 \mathbb{I}$ . Furthermore, these constraints do not require  $r' > r$ , as rewriting for example the first one as  $i \sum_{i=1}^{r'} \langle \dot{\psi}_\varphi | U |i\rangle \langle i| U |\psi_\varphi\rangle = 0$ , one can always resolve the identity with some basis vectors  $\sum_{i=1}^{r'} |i\rangle \langle i| = \sum_{i=1}^r |e_i\rangle \langle e_i|$  and define linearly independent Kraus operators  $\{K_i = \langle e_i | U |\psi_\varphi\rangle\}_{i=1}^r$  also fulfilling the necessary requirements.

Finally, we may conclude that  $\Lambda_\varphi$  is locally *quantum simulable* at  $\varphi$ , if it admits there a Kraus representation satisfying conditions (21) stated in the main text, which due to locality can be generated via (9) by some Hermitian  $r \times r$  matrix  $h$ . ■

## Appendix E. Finite- $N$ CE method as a semi-definite programming task

The finite- $N$  CE bound has been defined in (27) as

$$\mathcal{F}_N^{\text{CE}} = 4 \min_h \{ \|\alpha_{\tilde{K}}\| + (N-1) \|\beta_{\tilde{K}}\|^2 \}, \quad (\text{E.1})$$

where  $\|\cdot\|$  denotes the operator norm,  $\alpha_{\tilde{K}} = \sum_i \dot{K}_i^\dagger \dot{K}_i$  and  $\beta_{\tilde{K}} = i \sum_i \dot{K}_i^\dagger \tilde{K}_i$ . Given a channel  $\Lambda_\varphi$  from a  $d_{\text{in}}$ - to a  $d_{\text{out}}$ -dimensional Hilbert space and the set of its linearly independent Kraus operators ( $d_{\text{out}} \times d_{\text{in}}$  matrices)  $\{K_i\}_{i=1}^r$ , in order to compute  $\mathcal{F}_N^{\text{CE}}$ , we should minimize (E.1) over locally equivalent Kraus representations (9) of  $\Lambda_\varphi$  generated by all Hermitian,  $r \times r$  matrices  $h$ .

Basing on the results of [39], where the  $\beta_{\tilde{K}} = 0$  constraint (24) is also imposed on (E.1), we show that  $\mathcal{F}_N^{\text{CE}}$  can always be evaluated by means of semi-definite programming (SDP). Adopting a concise notation in which  $\mathbf{K}$  is a column vector containing the starting Kraus operators  $K_i$  as its elements, we can associate all locally equivalent Kraus representations  $\tilde{\mathbf{K}}$  in (E.1) with those generated by any  $h$  via  $\tilde{\mathbf{K}} = \mathbf{K}$  and  $\dot{\tilde{\mathbf{K}}} = \dot{\mathbf{K}} - ih\mathbf{K}$ . By constructing matrices ( $\mathbb{I}_d$  represents a  $d \times d$  identity matrix)

$$\mathbf{A} = \begin{bmatrix} \sqrt{\lambda_a} \mathbb{I}_{d_{\text{in}}} & \dot{\tilde{\mathbf{K}}}^\dagger \\ \dot{\tilde{\mathbf{K}}} & \sqrt{\lambda_a} \mathbb{I}_{r \cdot d_{\text{out}}} \end{bmatrix} \quad \mathbf{B} = \begin{bmatrix} \sqrt{\lambda_b} \mathbb{I}_{d_{\text{in}}} & \left( i \dot{\tilde{\mathbf{K}}}^\dagger \tilde{\mathbf{K}} \right)^\dagger \\ i \dot{\tilde{\mathbf{K}}}^\dagger \tilde{\mathbf{K}} & \sqrt{\lambda_b} \mathbb{I}_{d_{\text{in}}} \end{bmatrix}, \quad (\text{E.2})$$

which positive semi-definiteness conditions correspond respectively to

$$\alpha_{\tilde{K}} = \dot{\tilde{\mathbf{K}}}^\dagger \dot{\tilde{\mathbf{K}}} \leq \lambda_a \mathbb{I}_{d_{\text{in}}} \quad \beta_{\tilde{K}}^\dagger \beta_{\tilde{K}} = \tilde{\mathbf{K}}^\dagger \dot{\tilde{\mathbf{K}}} \dot{\tilde{\mathbf{K}}}^\dagger \tilde{\mathbf{K}} \leq \lambda_b \mathbb{I}_{d_{\text{in}}}, \quad (\text{E.3})$$

we rewrite (E.1) into the required SDP form

$$\mathcal{F}_N^{\text{CE}} = 4 \min_h \{ \lambda_a + (N-1) \lambda_b \}, \quad (\text{E.4})$$

s.t.  $\mathbf{A} \geq 0, \mathbf{B} \geq 0$ .

For the purpose of this paper we have implemented a semi-definite program using the CVX package for Matlab [102], which efficiently evaluates (E.4) given the set of Kraus operators and their derivatives of a generic channel  $\Lambda_\varphi$ . The fact that only  $\mathbf{K}$  and  $\dot{\tilde{\mathbf{K}}}$  are involved in (E.4) is a consequence of the QFI, and hence the bound  $\mathcal{F}_N^{\text{CE}}$ , being a local quantity.

Lastly, one should note that by slightly modifying the program in (E.4) we are able to also efficiently evaluate: the extended channel QFI (12), as  $\mathcal{F}[\Lambda_\varphi \otimes \mathcal{I}] = \mathcal{F}_{N=1}^{\text{CE}}$ ; and the asymptotic extended channel QFI (25),  $\mathcal{F}_{\text{as}}[\Lambda_\varphi \otimes \mathcal{I}] = \mathcal{F}_{\text{as}}^{\text{CE}}$ , by setting  $N = 1$  and imposing the  $\beta_{\tilde{K}} = 0$  constraint (24) as already pursued in [39].

## References

- [1] Leibfried D, Barrett M D, Schaetz T, Britton J, Chiaverini J, Itano W M, Jost J D, Langer C and Wineland D J 2004 *Science* **304** 1476–1478



- [2] Schmidt P O, Rosenband T, Langer C, Itano W M, Bergquist J C and Wineland D J 2005 *Science* **309** 749–752
- [3] Roos C F, Chwalla M, Kim K, Riebe M and Blatt R 2006 *Nature* **443** 316–319 ISSN 0028-0836
- [4] Ospelkaus C, Warring U, Colombe Y, Brown K R, Amini J M, Leibfried D and Wineland D J 2011 *Nature* **476** 181–184
- [5] Wasilewski W, Jensen K, Krauter H, Renema J J, Balabas M V and Polzik E S 2010 *Phys. Rev. Lett.* **104** 133601
- [6] Wolfgramm F, Cerè A, Beduini F A, Predojević A, Koschorreck M and Mitchell M W 2010 *Phys. Rev. Lett.* **105** 053601
- [7] Koschorreck M, Napolitano M, Dubost B and Mitchell M W 2010 *Phys. Rev. Lett.* **104** 093602
- [8] Mitchell M W, Lundeen J S and Steinberg A M 2004 *Nature* **429** 161–164
- [9] Nagata T, Okamoto R, O’Brien J L, Sasaki K and Takeuchi S 2007 *Science* **316** 726–729
- [10] Resch K J, Pregnell K L, Prevedel R, Gilchrist A, Pryde G J, O’Brien J L and White A G 2007 *Phys. Rev. Lett.* **98** 223601
- [11] Higgins B L, Berry D W, Bartlett S D, Mitchell M W, Wiseman H M and Pryde G J 2009 *New J. Phys.* **11** 073023
- [12] LIGO Collaboration 2011 *Nature Phys.* **7** 962–965
- [13] D J Wineland J J Bollinger W M I and Moore F L 1992 *Phys. Rev. A* **46** R6797–R6800
- [14] Bollinger J J, Itano W M, Wineland D J and Heinzen D J 1996 *Phys. Rev. A* **54** R4649–R4652
- [15] Bužek V, Derka R and Massar S 1999 *Phys. Rev. Lett.* **82** 2207–2210
- [16] Berry D W and Wiseman H M 2000 *Phys. Rev. Lett.* **85** 5098–5101
- [17] Giovannetti V, Lloyd S and Maccone L 2006 *Phys. Rev. Lett.* **96** 010401
- [18] Banaszek K, Demkowicz-Dobrzanski R and Walmsley I A 2009 *Nature Photon.* **3** 673–676
- [19] Giovannetti V, Lloyd S and Maccone L 2011 *Nature Photon.* **5** 222–229
- [20] Maccone L and Giovannetti V 2011 *Nature Phys.* **7** 376–377
- [21] Dowling J P 2008 *Contemp. Phys.* **49** 125–143
- [22] Andrè A, Sørensen A S and Lukin M D 2004 *Phys. Rev. Lett.* **92** 230801
- [23] Auzinsh M, Budker D, Kimball D F, Rochester S M, Stalnaker J E, Sushkov A O and Yashchuk V V 2004 *Phys. Rev. Lett.* **93** 173002
- [24] Huelga S F, Macchiavello C, Pellizzari T, Ekert A K, Plenio M B and Cirac J I 1997 *Phys. Rev. Lett.* **79** 3865–3868
- [25] Shaji A and Caves C M 2007 *Phys. Rev. A* **76** 032111



- [26] Dorner U 2012 *New J. Phys.* **14** 043011
- [27] Huver S D, Wildfeuer C F and Dowling J P 2008 *Phys. Rev. A* **78** 063828
- [28] Meiser D and Holland M J 2009 *New J. Phys.* **11** 033002
- [29] Dorner U, Demkowicz-Dobrzański R, Smith B J, Lundeen J S, Wasilewski W, Banaszek K and Walmsley I A 2009 *Phys. Rev. Lett.* **102** 040403
- [30] Demkowicz-Dobrzański R, Dorner U, Smith B, Lundeen J S, Wasilewski W, Banaszek K and Walmsley I A 2009 *Phys. Rev. A* **80** 013825
- [31] Kołodyński J and Demkowicz-Dobrzański R 2010 *Phys. Rev. A* **82** 053804
- [32] Knysh S, Smelyanskiy V N and Durkin G A 2011 *Phys. Rev. A* **83** 021804
- [33] Sarovar M and Milburn G J 2006 *J. Phys. A: Math. Gen.* **39** 8487
- [34] Ji Z, Wang G, Duan R, Feng Y and Ying M 2008 *IEEE Trans. Inf. Theory* **54** 5172–5185
- [35] Fujiwara A and Imai H 2008 *J. Phys. A: Math. Theor.* **41** 255304
- [36] Matsumoto K 2010 *ArXiv e-prints* 1006.0300
- [37] Hayashi M 2011 *Comm. Math. Phys.* **304** 689–709
- [38] Escher B M, de Matos Filho R L and Davidovich L 2011 *Nature Phys.* **7** 406–411
- [39] Demkowicz-Dobrzański R, Kołodyński J and Guță M 2012 *Nat. Commun.* **3** 1063
- [40] Chaves R, Brask J B, Markiewicz M, Kołodyński J and Acín A 2012 *ArXiv e-prints* 1212.3286
- [41] Acín A, Jané E and Vidal G 2001 *Phys. Rev. A* **64** 050302(R)
- [42] D’Ariano G M, Presti P L and Paris M G A 2001 *Phys. Rev. Lett.* **87** 270404
- [43] Chiribella G, D’Ariano G M, Perinotti P and Sacchi M F 2004 *Phys. Rev. Lett.* **93** 180503
- [44] Hotta M, Karasawa T and Ozawa M 2005 *Phys. Rev. A* **72** 052334
- [45] Sacchi M F 2005 *Phys. Rev. A* **71** 062340
- [46] D’Ariano G M, Sacchi M F and Kahn J 2005 *Phys. Rev. A* **72** 052302
- [47] Chiribella G, D’Ariano G M and Perinotti P 2008 *Phys. Rev. Lett.* **101** 180501
- [48] Sedlák M and Ziman M 2009 *Phys. Rev. A* **79** 012303
- [49] Bisio A, D’Ariano G M, Perinotti P and Sedlák M 2012 *Phys. Rev. A* **85** 032333
- [50] Pirandola S 2011 *Phys. Rev. Lett.* **106** 090504
- [51] Pirandola S, Lupo C, Giovannetti V, Mancini S and Braunstein S L 2011 *New J. Phys.* **13** 113012
- [52] Nair R 2011 *Phys. Rev. A* **84** 032312
- [53] Nair R and Yen B J 2011 *Phys. Rev. Lett.* **107** 193602
- [54] Breuer H P and Petruccione F 2002 *The Theory of Open Quantum Systems* (Oxford University Press)
- [55] Andersson E, Cresser J D and Hall M J W 2007 *J. Mod. Opt.* **54** 1695

- [56] Matsuzaki Y, Benjamin S C and Fitzsimons J 2011 *Phys. Rev. A* **84** 012103
- [57] Chin A W, Huelga S F and Plenio M B 2012 *Phys. Rev. Lett.* **109** 233601
- [58] Szankowski P, Chwedeńczuk J and Trippenbach M 2012 *ArXiv e-prints* 1212.2528
- [59] Kay S M 1993 *Fundamentals of Statistical Signal Processing: Estimation Theory* (Prentice Hall)
- [60] Nielsen M A and Chuang I L 2000 *Quantum Computing and Quantum Information* (Cambridge University Press)
- [61] Bengtsson I and Życzkowski K 2006 *Geometry of quantum states: an introduction to quantum entanglement* (Cambridge University Press)
- [62] Helstrom C W 1976 *Quantum detection and estimation theory* (Academic Press)
- [63] Holevo A S 1982 *Probabilistic and Statistical Aspects of Quantum Theory* (North Holland)
- [64] Braunstein S L and Caves C M 1994 *Phys. Rev. Lett.* **72** 3439–3443
- [65] Nagaoka H 2005 *On Fisher Information of Quantum Statistical Models* (World) chap 9, pp 113–125
- [66] Tóth G and Petz D 2013 *Phys. Rev. A* **87** 032324
- [67] Yu S 2013 *ArXiv e-prints* 1302.5311
- [68] Fujiwara A 1994 *Math. Eng. Tech. Rep.* **94** 94–10
- [69] Genoni M G, Paris M G A, Adesso G, Nha H, Knight P L, and Kim M S 2012 *ArXiv e-prints* 1206.4867
- [70] Fujiwara A 2001 *Phys. Rev. A* **63** 042304
- [71] Braunstein S L, Caves C M and Milburn G 1996 *Ann. Phys.* **247** 135 – 173
- [72] Aharonov Y, Massar S and Popescu S 2002 *Phys. Rev. A* **66** 2002
- [73] Ulam-Orgikh D and Kitagawa M 2001 *Phys. Rev. A* **64** 052106
- [74] Caves C M 1981 *Phys. Rev. D* **23** 1693–1708
- [75] Greenberger D M, Horne M and Zeilinger A *Bells Theorem, Quantum Theory, and Conceptions of the Universe* (Dordrecht, The Netherlands: Kluwer Academic Publishers)
- [76] Lee H, Kok P and Dowling J P 2002 *J. Mod. Opt.* **49** 2325
- [77] Demkowicz-Dobrzański R, Banaszek K and Schnabel R 2013 *ArXiv e-prints* 1305.7268
- [78] Monras A and Paris M G A 2007 *Phys. Rev. Lett.* **98** 160401
- [79] Adesso G, Dell’Anno F, Siena S D, Illuminati F and Souza L A M 2009 *Phys. Rev. A* **79** 040305(R)
- [80] Crowley P J D, Datta A, Barbieri M and Walmsley I A 2012 *ArXiv e-prints* 1206.0043
- [81] Hotta M, Karasawa T and Ozawa M 2006 *J. Phys. A: Math. Gen.* **39** 14465

- [82] Fujiwara A and Imai H 2003 *J. Phys. A: Math. Gen.* **36** 8093–8103
- [83] Fujiwara A 2004 *Phys. Rev. A* **70** 012317
- [84] Frey M, Collins D and Gerlach K 2011 *J. Phys. A: Math. Theor.* **44** 205306
- [85] Hyllus P, Pezzé L and Smerzi A 2010 *Phys. Rev. Lett.* **105**(12) 120501
- [86] Hofmann H F 2009 *Phys. Rev. A* **79** 033822
- [87] Zwiernik M, Pérez-Delgado C A and Kok P 2010 *Phys. Rev. Lett.* **105** 180402
- [88] Anisimov P M, Raterman G M, Chiruvelli A, Plick W N, Huver S D, Lee H and Dowling J P 2010 *Phys. Rev. Lett.* **104** 103602
- [89] Giovannetti V and Maccone L 2012 *Phys. Rev. Lett.* **108** 210404
- [90] Pezzé L and Smerzi A 2008 *Phys. Rev. Lett.* **100** 073601
- [91] Giovannetti V, Lloyd S and Maccone L 2012 *Phys. Rev. Lett.* **108** 260405
- [92] Kahn J and Guță M 2009 *Comm. Math. Phys.* **289** 597–652
- [93] Sørensen A S and Mølmer K 2001 *Phys. Rev. Lett.* **86** 4431–4434
- [94] Jarzyna M and Demkowicz-Dobrzański R 2013 *ArXiv e-prints* 1301.4246
- [95] Chiribella G, D’Ariano G M and Sacchi M F 2005 *Phys. Rev. A* **72** 042338
- [96] Boixo S and Somma R D 2008 *Phys. Rev. A* **77** 052320
- [97] Teklu B, Olivares S and Paris M G A 2009 *J. Phys. B: At., Mol. Opt. Phys.* **42** 035502
- [98] Demkowicz-Dobrzański R 2011 *Phys. Rev. A* **83** 061802(R)
- [99] Hall M J W and Wiseman H M 2012 *New J. Phys.* **14** 033040
- [100] Nair R 2012 *ArXiv e-prints* 1204.3761
- [101] Datta A, Zhang L, Thomas-Peter N, Dorner U, Smith B J and Walmsley I A 2011 *Phys. Rev. A* **83** 063836
- [102] Grant M and Boyd S 2012 Cvx: Matlab software for disciplined convex programming URL <http://cvxr.com/cvx/>